JOURNAL OF GEOPHYSICAL RESEARCH, VOL. 95, NO. D11, PAGES 18,705–18,721, OCTOBER 20, 1990

The Effect of Summer Tropical Heating on the Location and Intensity of the Extratropical Westerly Jet Streams

SONG YANG

Atmospheric and Environmental Research, Inc., Cambridge, Massachusetts

PETER J. WEBSTER

Department of Meteorology, Penn State University, University Park

The role of the summer hemisphere tropical diabatic heating on the location and magnitude of the winter hemisphere subtropical and extratropical westerly jet streams is studied. In particular, the relationships between the extratropical zonal wind, the subtropical meridional wind and the tropical outgoing longwave radiation (OLR) patterns are examined. It is found that the heating field, the cross-equatorial meridional wind, and the winter zonal wind maxima are closely linked on annual and interannual time scales. These factors indicate that the adjacent hemisphere heating is at least as important as the northern hemisphere orography in determining the location and magnitude of the westerly jet streams. Credence is added to this conclusion by noting the similar associations between the northern hemisphere heating pattern and the location and variations of the southern hemisphere jet streams which are less clearly associated with orography. Furthermore, interannual changes in the location and magnitude of the westerly jet streams are closely related to the El Niño/Southern Oscillation (ENSO) phenomenon. Thus, in addition to the well known relationship between ENSO and the near-equatorial or symmetric zonal circulation, there is a strong association on the same time scale in the cross-equatorial flow or asymmetric components about the equator.

1. INTRODUCTION

Over the past decade or so it has become clear that the meteorology of the two hemispheres is interactive on time scales from the synoptic to the interannual. For example, *Webster and Holton* [1982] have shown that events in one hemisphere, on such a broad frequency band, could interact through the "westerly duct" of the tropical upper troposphere to influence the other hemisphere. This region of strong westerlies, referred to as "the westerly duct" by Webster and Holton, spans the equator joining the extratropical westerlies of each hemisphere. In part, the equatorial westerlies are produced by the longitudinal heating gradients along the equator and by the resultant Walker circulation [see *Webster*, 1973; *Frederiksen and Webster*, 1988]. *Chang* [1977] has suggested that the differential heating in the adjacent hemispheres may project onto the very low frequency equatorially trapped "odd" modes, helping to explain such phenomena as the asymmetric monsoon circulations. Thus, for these modes, any alteration of the heating gradient occurring on either side of the equator will affect the structure of the mode even in the adjacent hemisphere. For higher frequency phenomena, *Webster and Chang* [1988] and *Zhang and Webster* [1989] have shown that the longitudinal variations in the equatorial flow induced by the Walker circulation severely modify the characteristics of both equatorial and extratropical transient modes. Furthermore, they speculated that the basic state variability determines, to a large extent, the manner in which the extratropics and the tropics jointly interact.

Paper number 90JD01250.
0148-0227/90/90JD-01250$05.00

Based upon these observational and theoretical realizations, the question arises as to whether it is feasible that specific phenomena in one hemisphere can be influenced by specific forcing in the other. There are clear examples of variations of heating occurring on interannual time scales but what effect do they have on remote events in the other hemisphere? Along the same lines, we may ask a specific question that is central to the subject of this paper and which also supplies a specific test for the existence of an interhemispheric linkage. Do relationships exist between the location and the intensity of the winter hemisphere jet streams and the forcing due to heating in the other hemisphere?

There are rather important reasons why we might ask the question of what causes the variation of the jet stream location and intensity. A number of studies [e.g., *Blackmon, et al.*, 1977] have shown that the jet streams are source regions of extratropical storms. Thus, variations in the jet stream position and intensity may have a significant impact on the weather of the winter hemisphere. However, the processes which create the jet streams, or define their locations and intensities, together with other mean features of the extratropics, have long been the subject of considerable controversy.

1.1. *Relative Role of Orography and Heating in Determining the Location and Intensity of the Mean Structure of the Extratropics*

Whether orographic or thermal forcing is the dominant process in determining the location and magnitude of extratropical stationary waves has been the subject of much discussion and debate. For example, *Charney and Eliassen* [1949], *Bolin* [1950], *Manabe and Terpstra* [1974], *Held* [1983], *Wallace* [1983], *Jacqmin and Lindzen* [1985], and many others, claimed that the effect of topography is primary and instrumental in forcing stationary waves. Clearly, there is theoretical evidence to support such an impor-

tant role for orography. For example, the study of *Held* [1983] using a hemispheric barotropic model with only orographic forcing found zonal wind maxima downstream of the major northern hemisphere orographic features. *Chen and Trenberth* [1988], using a steady state hemispheric model, found solutions that matched the mean structure of the northern hemisphere by including a feedback which allowed the perturbations produced by the heating differentials to interact with the orography. However, the model was hemispheric. Thus, both the Held and the Chen and Trenberth studies precluded the possibility of cross-equatorial flow and inter-hemispheric interaction through the geographic limitations of their models. Their analyses were not conducted for the southern hemisphere where it may have been difficult to predict the general position and the very large seasonal swings in the jet streams by orographic effects alone (see Figure 1 and the discussion in section 1.2).

There have been other studies, however, that have found a much greater role for the differential heating, but again from a hemispheric perspective. *Smagorinsky* [1953], *Kasahara and Washington* [1971], *Rong-hui and Gambo* [1982], among others, argued that the extratropical thermal forcing (such as produced by land-sea contrast) is a dominant perturber of the mean flow.

Collectively, the result of the studies discussed above indicate that there is still great uncertainty about the relative role of heating and orography of the large scale circulation of the extratropics. This has lead to attempts to relegate the various roles of heating and orography in the general circulation. For example, in his diagnostic study, *Wallace* [1983] stated that::

> ...it is possible to ascribe the dominant features associated with the observed stationary waves to specific processes which are quite well understood, and whose importance is widely acknowledged:....[1] orographic forcing by the Himalayas, Rockies and Antarctica which determine the positions of the major features in the upper level geopotential height field during wintertime [and the high latitude pattern of the Southern hemisphere during summer as well], and...[2] thermal forcing associated with land-sea contrasts which account for the monsoon circulations of the summer hemisphere equatorward of the jetstream, as well as an assortment of shallow features at high latitudes of the winter hemisphere...

Wallace, thus, implied that there were clearly defined geographical regions where, selectively, orographic forcing (the extratropics) and thermal forcing (the tropics and subtropics) were dominant. Remote effects, such as "... remote forcing by Rossby wave propagation..." were relegated to a secondary importance.

While the *Wallace* [1983] study concentrated on the very long term mean structure of the major features of the atmosphere, considerable attention has been focused on the anomalous response of the extratropical westerlies and jet streams to the interannual variations of tropical heating associated with the Southern Oscillation [e.g., *Bjerknes*, 1966, 1969; *Paegle et al.*, 1979; *Opsteegh and Van den Dool*; 1980, *Hoskins and Karoly*, 1981; *Webster*, 1981, 1982 and *Simmons*, 1982, among others]. More direct links between

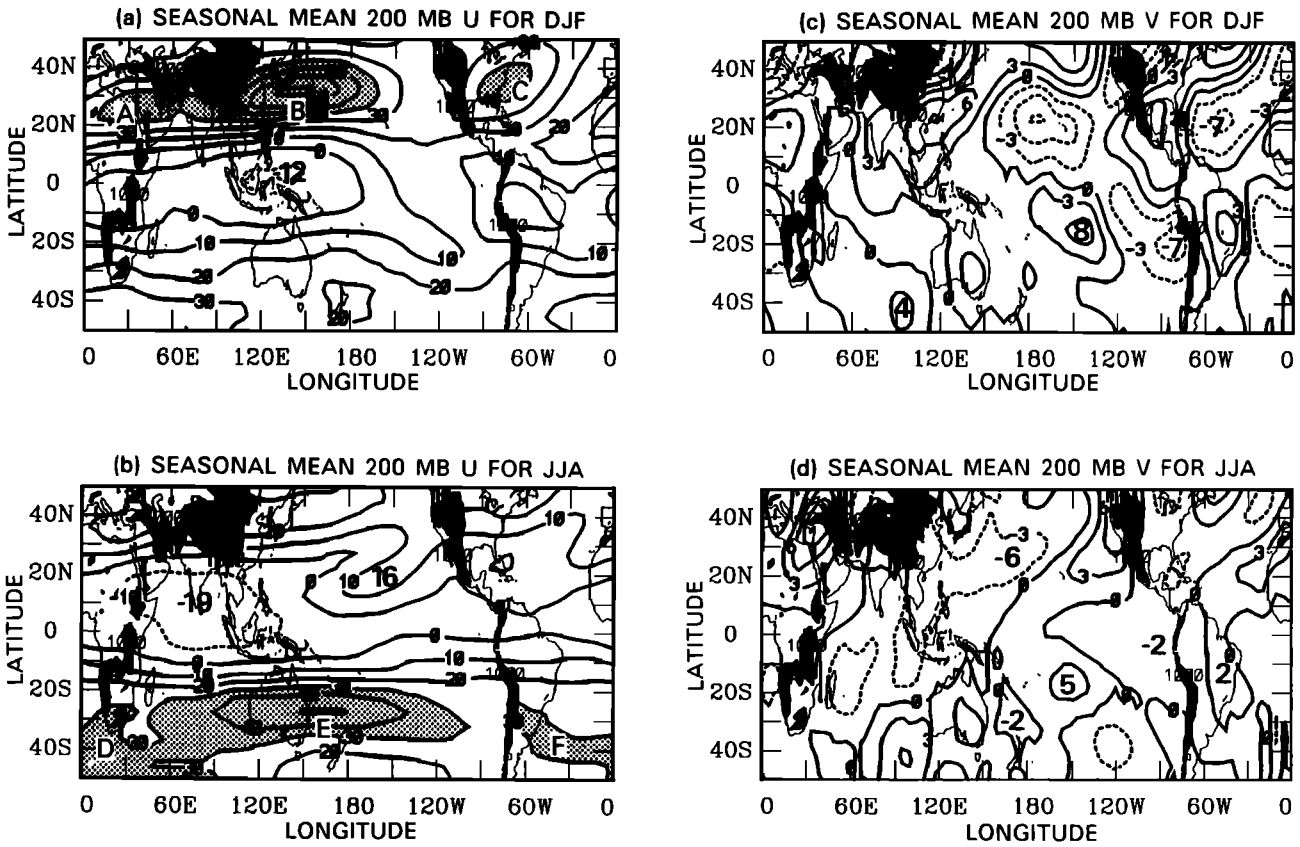

Fig. 1. Latitude-longitude distributions of (a) 200-mbar U for DJF, (b) 200-mbar U for JJA, (c) 200-mbar V for DJF and (d) 200-mbar V for JJA. Dates are averaged between 1968 and 1988 and units are in m s^{-1}. The major mountain ranges (≥ 1000 m) are shaded and the regions of maximum westerly winds (≥ 40 m s^{-1} in (a) and ≥ 30 m s^{-1} in (b)) are stippled.

the mean circulation and the tropical heating were seen by *Ramage* [1968] and *Krishnamurti, et al.*, [1973] and *Krishnamurti* [1979]. The Southern Oscillation, originally defined by *Walker* [1924], describes the oscillation in surface pressure between the western Pacific and eastern Pacific Oceans. (The Southern Oscillation Index (SOI) is approximately the normalized pressure difference between Tahiti and Darwin. The difference shows a low amplitude variation with about a 2–4 year period.)

In particular, *Krishnamurti, et al.*, [1973] and *Krishnamurti* [1979] showed an apparent association between three tropical heating centers and the three winter northern hemisphere winter jet maxima. Specifically, *Krishnamurti* [1979, p. 325] stated that:

> ...The ageostrophic flows in the southwesterly branch of the subtropical jet is, in fact, seen to originate from the ITCZ. This air moves northeastwards crossing towards lower pressure, giving rise to strong winds in the ridges of the subtropical jet stream of winter. There exists a one-to-one relationship between the three ridges of the subtropical jet stream and the following three well-known rainfall belts of the northern winter season: [i] The Indonesian-southern Malaysia region, [ii] Equatorial central Africa, and, [iii] The Amazon and the northwestern part of South America... The three major tropical rainfall belts provide a link between the northern and southern hemisphere phenomena...

Lau and Boyle [1987] studied the effect of the tropical diabatic heating on the tropical and extratropical large-scale atmospheric winter circulation. They found that the changes in heating over the western and central Pacific Ocean were accompanied by significant changes of the global atmospheric circulation, including the East Asia jet stream.

However, in spite of the work mentioned above, there has been little emphasis placed on the importance of the cross-equatorial heating-jet association. The prevailing thoughts regarding the forcing of the mean circulation appear to agree with the opinion of Wallace, as paraphrased above, with the interannual variation of this mean flow reflecting variations in the Southern Oscillation.

1.2. *Juxtapositions of the Extratropical Jet Streams with Local Orography and Remote Heating: Associations and Paradoxes*

Figure 1 shows a simplified version of the latitude-longitude distributions of the mean 200-mbar zonal and meridional wind components [$\bar{U}$ and $\bar{V}$, m s^{-1}] for DJF [December, January and February] and JJA [June, July and August]. The data used come from the National Meteorological Center [NMC] data set which is described in section 2. The shaded regions show the orographic features and the stippled regions show the maximum westerly zones in the extratropics.

Figure 1 reveals several interesting features. In the northern hemisphere winter, each of the extratropical westerly jet streams (A, B, and C) is downstream of a major orographic feature, specifically, to the east of the Alps, Himalayas and Rockies, respectively. The relative location of the northern hemisphere mountains and the jet centers would seem to support the hypothesis that there was a direct relationship between the location of the jet streams and the orography. However, a more detailed examination of the figure indicates that this simple hypothesis may have some problems, or, at least, that it may not be general. The hypothesis fails in at least one instance. In the southern hemisphere, the major westerly jet stream (E) is less obviously associated with orography. The only orographic feature in the southern hemisphere with a low order scale is Antarctica which has been thought to produce the long wave structure [e.g., *Wallace*, 1983; *James*, 1988]. Furthermore, the major southern hemisphere jet stream changes its location radically from one season to another. Also, in the northern hemisphere summer, the jet stream locations vary substantially from their winter locations and thus appear less associated with orography.

Figure 2a shows time-longitude plots of $\bar{U}$ averaged between 25°N and 35°N, 5°N and 5°S and 25°S, and 35°S for DJF and provides an indication of the interannual variation of the large scale upper tropospheric wind maxima over the globe. Considerable variability is apparent. In the equatorial belt, the winds oscillate from periods of wind minimum along the equator to periods of wind maxima. Generally, the minima are associated with negative Southern Oscillation Index (SOI) and the maxima with positive SOI. The seasonal mean values of the SOI are shown in each panel of the figure for each season. At higher latitudes in both hemispheres, near-simultaneous variations in the zonal wind field occur. Figure 2b shows the same set of sections but for JJA. Large interannual excursions appear in the wintertime southern hemisphere with an apparent relationship to the SOI. With the SOI << 0, the westerly maximum intensifies and moves eastward. Although the winds are much lighter in the summer hemisphere (as shown in Figure 1), the jet maxima, although fairly weak, is further poleward than the 25°–35°N section. However, considerable variability, again apparently associated with the SOI, is apparent in the vicinity of the mid-Pacific trough which will be emphasized in the following sections.

Figure 2c shows the simultaneous correlations of the $\bar{U}$ field between 5°N-5°S and 25°N-35°N (upper panel), between 5°N-5°S and 25°S-35°S (middle panel), and between 25°N-25°N and 25°S-35°S (lower panel). The longitude belts corresponding to the DJF tropical westerlies are marked with heavy lines. Correlations passing the 95% significance level are shaded. In both DJF and JJA, the strongest correlations occur over the central-eastern Pacific Ocean, where tropical westerlies prevail in DJF and relatively weak tropical easterlies appear in JJA. The correlations between the tropics and extratropics are stronger in DJF than in JJA in the northern hemisphere, although they are similar in magnitude in both seasons in the southern hemisphere. A strong negative correlation is shown clearly over the central Pacific Ocean in the upper and middle panels; stronger (weaker) equatorial westerlies and weaker (stronger) equatorial easterlies are accompanied by weaker (stronger) extratropical westerlies in both hemispheres. Thus, an in-phase change occurs in the extratropical westerlies over the central Pacific Ocean of both hemispheres. Note, too, the strong positive correlations in the lower panel. Although somewhat weaker, negative tropics-extratropics correlations are found over Asia in DJF and over the southern Indian Ocean in JJA, which show the relationship of the extratropical westerly jet streams to the tropical easterlies. In turn, the tropical easterlies are closely associated with the diabatic heating maximum over the eastern Indian Ocean and the western Pacific Ocean, as shown in the following sections. In summary, the maximum cross-equatorial correlation occurs in the region of *Webster and Holton's* [1982] "westerly duct". Also, substantial correlations, although relatively weaker, occur between the strength of the equatorial easterlies and the extratropical westerlies.

The variations shown in Figure 2 are difficult to ascribe to orography, at least in a simple manner. The ascription is difficult because of the seasonal differences in the jet stream locations and because of the very large interannual variations. Such an argument would have to be rather convoluted. Somehow, the mean zonally averaged flow or an anomalous long wave pattern

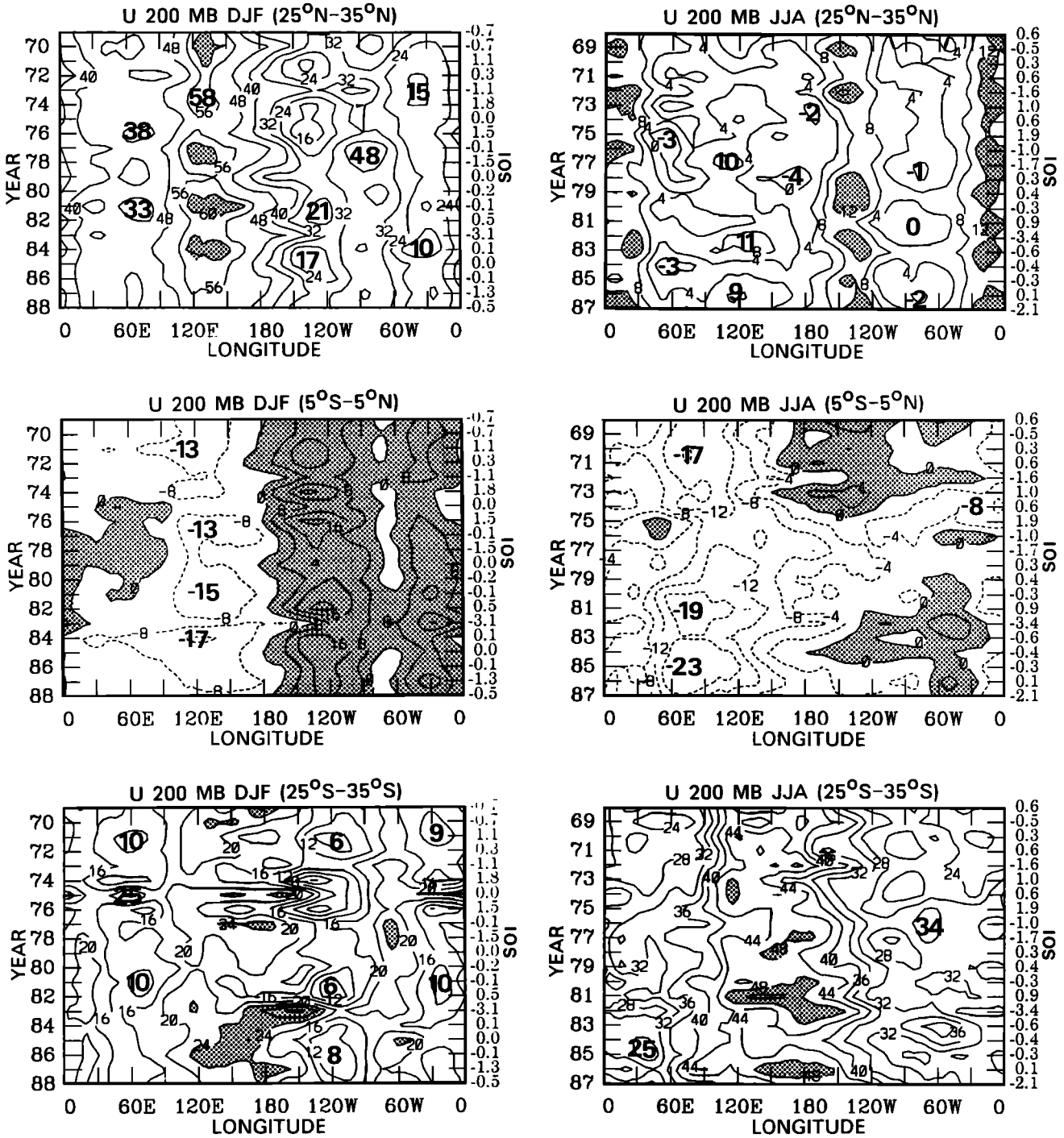

Fig. 2a. Longitude-time diagrams of the $\bar{U}$-field averaged between December and February (DJF), and 25°–35°N (upper panel; stippling denotes area where $U \geq 60$ m s^{-1}), 5°N-5°S (middle panel; stippling denotes area where $U \geq 0$) and 25°S-35°S (lower panel; stippling denotes area where $U \geq 24$ m s^{-1}) from the DJF of 1968/1969 (represented by 69) through the DJF of 1987/1988 (represented by 88). (Units, m s^{-1}.)

Fig. 2b. Same as Figure 2a except for the June through August (JJA) fields. Regions of $U \geq 12$ m s^{-1}, $U \geq 0$, $U \geq 48$ m s^{-1} are stippled at the upper, middle and lower panels, respectively.

must contain the interannual variability produced, perhaps, by heating variation. This adjusted pattern, in turn, would have to produce an anomalous response with the orographic features in the manner of *Chen and Trenberth* [1988], discussed above.

1.3. *An Alternative Hypothesis: Testing the Relationship Between Summer Heating and the Location of the Winter Extratropical Jetstreams*

Figures 1 and 2 indicate substantial variability and correlation on interannual and annual time scales between major circulation features of the atmosphere. In particular, there appear to be common relationships between jet positions, cross-equatorial flow and orographic features. Noting the absence of mountain in the

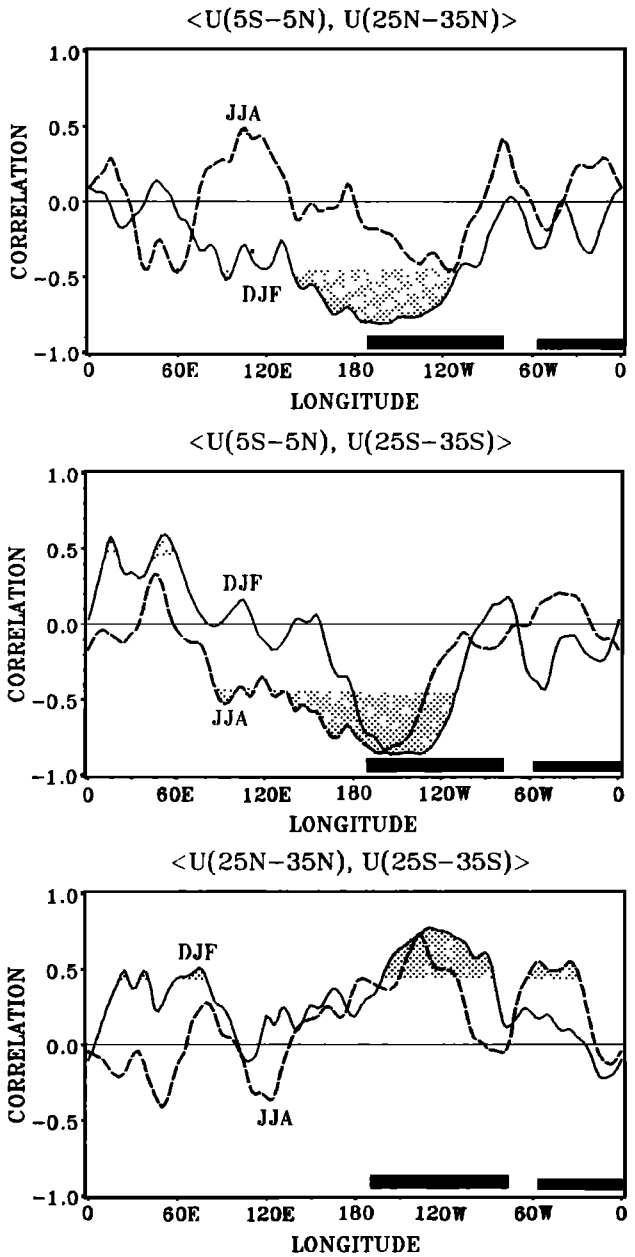

Fig. 2c. Simultaneous correlations (for both DJF and JJA) of the U field between 5°N-5°S and 25°N-35°N (upper panel), between 5°N-5°S and 25°S-35°S (middle panel), and between 25°N-35°N and 25°S-35°S (lower panel). Values which pass the 95% significance level (± 0.44) are shaded. Thick dark bars indicate the longitudinal spans of equatorial westerlies in DJF. Easterlies prevail over all locations along the equator in JJA.

southern hemisphere and the large annual change of the jet stream, it would appear that a comparison of mechanisms between the two hemispheres may be profitable. An immediate question is whether there are any common features of the jet streams of both hemispheres which might suggest that they may have a common physical basis. An alternative question is whether or not the southern hemisphere jet streams are created and maintained by different mechanisms than those which force their northern hemisphere counterparts.

It will be shown that there is a common characteristic between the jet streams of both hemispheres. This is that each winter hemisphere jet is poleward of a region of maximum heating located in the summer hemisphere. The idea of such a relationship is not entirely new. *Krishnamurti et al.*, [1973] speculated that the three stationary waves of the subtropical jet stream in the northern hemisphere may be related to the three major tropical convective regions [i.e., South Africa, South America, and Indonesia]. The distributions of convection for Krishnamurti's study were inferred from brightness data [*Sadler*, 1970] and the position of the jets inferred from analyses of 200-mbar stream function fields.

With current data sets, the hypothesis of Krishnamurti et al., (the relationship between remote heating and the jet stream location) is now much easier to test. There exist better and longer term data sets including multi-year outgoing longwave radiation [OLR] fields and equally long descriptions of the dynamics and thermodynamics. These data sets, described in the next section, will be used to test how robust the hypothetical relationship is throughout the data period. Clearly, if Krishnamurti's hypothesis is true, it should be expected that the interannual variability of the jet streams of the winter hemisphere would correspond to the variations in the tropical heating of the summer hemisphere. That is, periods with anomalous heating in the adjacent hemisphere should correspond to the anomalous location and magnitude of the jets in the other. In the following sections we examine these relationships.

2. DESCRIPTION OF THE DATA

The data sets used in this study originate from the operational tropical objective-analyses of NMC. They consist of monthly mean values of the zonal and meridional wind components at six levels (1000, 850, 700, 500, 300 and 200-mbar) from March 1968 to February 1988 and monthly mean values of OLR but from June 1974 to February 1988. Within the data sets, there are some missing data. For example, no 200-mbar winds are available for October and November 1972 and the OLR data is missing from March to December 1978. Therefore, the DJF mean values of the OLR for 1978/1979 were obtained using data from only January and February 1979. OLR values for JJA of 1978 are interpolated from the OLR fields of JJA of 1977 and 1979. The data is set on a 72x23 Mercator longitude-latitude grid. The longitudinal spacing is 5°. The latitudinal spacing varies from 5° at the equator to 3.5° at the southern and northern boundaries which are located at 48.1°S and 48.1°N.

As these NMC data sets are the product of an operational system, a number of different objective analysis and initialization schemes have been used in their production through the years. As indicated by *Arkin* [1982], the different schemes will affect, in particular, the magnitude of the divergent part of the wind field. Unfortunately, we are forced to live with these deficiencies. More details about the data sets can be found in *Arkin* [1982] and *Arkin and Webster* [1985] . A critical evaluation of the NMC sets has been undertaken by *Trenberth and Olson* [1988].

3. ANNUAL VARIABILITY OF THE HEATING FIELD

The long term mean annual distributions of OLR from 1974 to 1988 (i.e., the averaged values of all of the available monthly mean data of the period) are shown in Figure 3a. Three heat sources (i.e., OLR minima < 220 W m^{-2}, hatched) and three heat sinks (i.e., OLR maxima > 260 W m^{-2}, stippled) are apparent in the tropical regions. We make the association between OLR maxima (minima) and heat sink (source) for the following reasons. OLR minima (i.e., < 220-230 W m^{-2}) are usually associated with

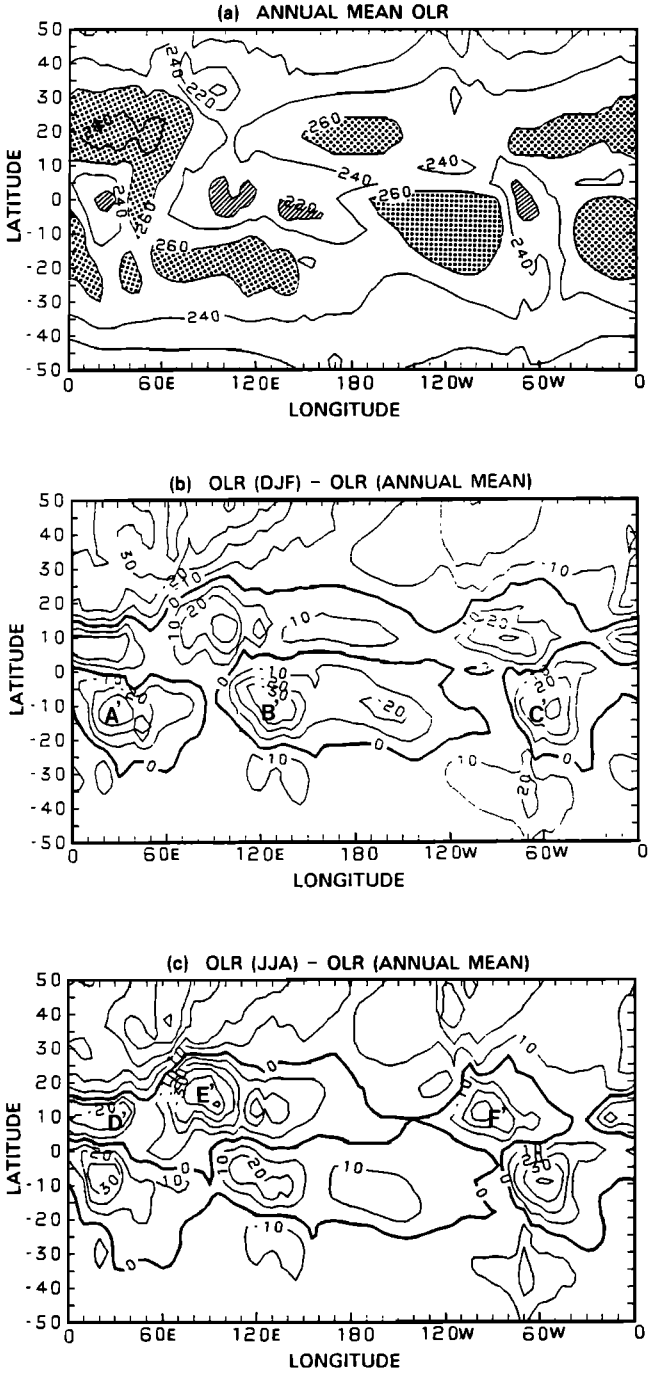

Fig. 3. Latitude-longitude distributions of (a) the annual mean OLR computed from 1974 through 1988, (b) the difference of DJF mean and annual mean OLR fields and (c) the difference of JJA mean and annual mean OLR fields. Units are in W m^{-2}.

deep precipitating cloud systems, at least in the tropics, and hence, with latent heat release. Furthermore, OLR minima, and hence, cloudy regions, are associated with a vertical radiative flux convergence relative to larger OLR or clearer regions [*Ramanathan*, 1987]. Thus, the horizontal latent and radiative heating gradients are in phase and directed from OLR maxima to OLR minima. The strongest and broadest heat source is over the eastern Indian Ocean and the western Pacific Ocean, overlaying Indonesia and the warm pool regions of the tropical oceans. The other two heat sources, smaller in spatial extent, correspond to the tropical continental regions of Africa and the Americas, respectively. On the other hand, the strongest and broadest heat sink is over the central-eastern Pacific Ocean, overlaying the colder sea surface temperature [SST] regions of the tropical oceans and corresponding to the large subsident regions of the Walker circulation. The other two heat sinks are over the Atlantic Ocean and the western Indian Ocean, respectively, but they are somewhat weaker and less extensive.

The differences between the two seasonal [DJF and JJA] means and the annual mean provide an estimate of the magnitude of the annual cycle. These differences are shown in Figures 3b and 3c, respectively. During DJF, the OLR difference field is negative in the tropical-subtropical regions in the northern hemisphere and positive in the southern hemisphere. During JJA, the opposite situation is found. Thus, a distinct annual latitudinal migration exists in the tropical heating band. The difference fields show a relative gradient in the north-south direction of about 60 W m^{-2} over a 20°–30° latitude band. The longitudinal gradient is much smaller, with maximum values of about 20 W m^{-2} over 60° of longitude. It can also be noticed that the annual changes of the heating field are regional in nature, being relatively small over the oceans but very large in the continental areas, especially in the monsoon regions. An exception to this rule occurs in the central equatorial Pacific Ocean to the south of the equator. There, the changes from one season to the next are about 30 W m^{-2}. Probably, these changes echo the different strength of the South Pacific convergence band discussed by *Streten* [1973], as it waxes and wanes from summer to winter.

From Figures 1 and 3, it can be seen that the heat source-sink pattern corresponds in longitude with the three core structure of the extratropical winter westerly jet streams. During DJF, all the winter extratropical westerly jet streams (A, B, and C in Figure 1a) in the northern hemisphere are poleward of the maximum tropical heating centers (A', B', and C' in Figure 3b) in the southern hemisphere. Similar associations between the heating in the northern hemisphere and the jet maxima in the southern hemisphere can be found for JJA. Then, the three maximum westerly centers (D, E, and F in Figure 1b) in the southern hemisphere, although more difficult to discern, are aligned with the three maximum heating centers (D', E', and F' in Figure 3c) in the northern hemisphere. Special attention should be given to the fact that the Australian jet stream (E), which is the strongest jet over the entire globe during JJA is not associated with a major mountain range. E is located just east of the longitudes of the Asian monsoon heating, which, in turn, is the strongest diabatic heating center. Therefore, correspondence in longitude of the jets and the heating centers and their in-phase annual changes suggest either a clear association between the jets and the heating field or a considerable coincidence. Figures 1 and 3 show another feature which adds credence to the assertion about the annual heating-jet relationship. That is, the entrance regions of the winter hemisphere jet streams are all downstream of strong upper-tropospheric cross-equatorial flows which are apparently associated with the outflow from the strong summer heating centers.

4. HEATING-JET RELATIONSHIP AND ENSO PHENOMENA

The possibility of the longitudinal alignment of the low latitude heating and the extratropical jet stream centers being merely a coincidental juxtaposition would be reduced if the temporal variations of each component were found to be common. Indeed, the

tropical heating field changes significantly from year to year corresponding to the variations of the SOI [e.g., *Bjerknes*, 1966, 1969]. (The SOI values shown here and henceforth are from the *Climate Diagnostics Bulletin*, a monthly climate summary published by the Climate Analysis Center of the NOAA National Meteorology Center, Washington, DC 20233.) Thus, we will now examine the relationships between the variations of the extratropical westerly jet streams and tropical heating in El Niño [SOI << 0] and La Niña [SOI >> 0] years. Table 1 shows the El Niño and La Niña winters and summers for the period from 1968 to 1988 used in the study. The criterion for their choice is that the absolute values of the seasonal means of the SOI [i.e., the average of the three monthly values] are not less than 0.5.

4.1. *Interannual Variability of OLR, $\bar{U}$, and $\bar{V}$ During Winter*

Figure 4 shows the mean OLR patterns for two El Niño winters (DJF of 1982/1983 and 1986/1987) and two La Niña winters (DJF of 1975/1976 and 1981/1982). The seasonal mean values of the SOI for DJF of 1982/1983, 1986/1987, 1975/1976 and 1981/1982 are -3.1, -1.3, 1.5 and 0.5, respectively. It should be pointed out that, in order to have an equal number of El Niño and La Niña years for which there are OLR data, we pick the two La Niña winters of 1975/1976 and 1981/1982. Note, though, that the data are available for another El Niño winter (197/1978) which were not used. There are significant differences in OLR distributions between the two extremes. The largest change occurs over the eastern Indian Ocean and the western Pacific Ocean where the OLR minimum moves eastward to the central Pacific Ocean when SOI < 0. The transposition of the minimum is much more apparent in Figure 4c, where the OLR decreases by 60 W m^{-2} in the central Pacific Ocean and increases by 30 W m^{-2} near Indonesia during the El Niño winters. Between Figures 3b and 4c, we can see that the magnitude of the interannual anomalous heating gradient is about the same as that of the annual cycle, although the orientation of the gradient is very different. In this case, the major changes in gradient are oriented longitudinally. However, the eastward migration of the OLR minimum from Indonesia to the central Pacific Ocean during the El Niño winters increases the latitudinal heating gradient east of 160°E and decreases the gradient west of 160°E as well. Note that to the north and south of the anomalous heating along the equator, the OLR changes are of the opposite sign. Clearly, the changes associated with the El Niño/Southern Oscillation [ENSO] phenomenon are not restricted to the tropics.

The corresponding mean 200-mbar $\bar{U}$ field and its differences are shown in Figure 5. In the tropics, there is a general weakening of the westerlies in the central-eastern Pacific Ocean during the El Niño winters, although the westerlies strengthen over the Atlantic Ocean. These changes appear consistent with the variations of the longitudinal heating gradient shown in Figure 4c. There are also very significant changes in the subtropical and extratropical westerlies. When SOI < 0, the westerlies over both hemispheres increase in magnitude and the maximum centers are located further eastward. Note that the maximum differences exist in the longitude band extending over the central and eastern

TABLE 1. El Niño and La Niña Years (|SOI| ≥ 0.5)

Season	SOI ≥ 0.5	SOI ≤ 0.5
DJF	1970/1971	1968/1969
	1975/1976	1972/1973
	1973/1974	1982/1983
	1981/1982	1969/1970
		1977/1978
		1986/1987
JJA	1968	1969
	1973	1976
	1975	1982
	1971	1987
	1974	1972
	1981	1977
		1983

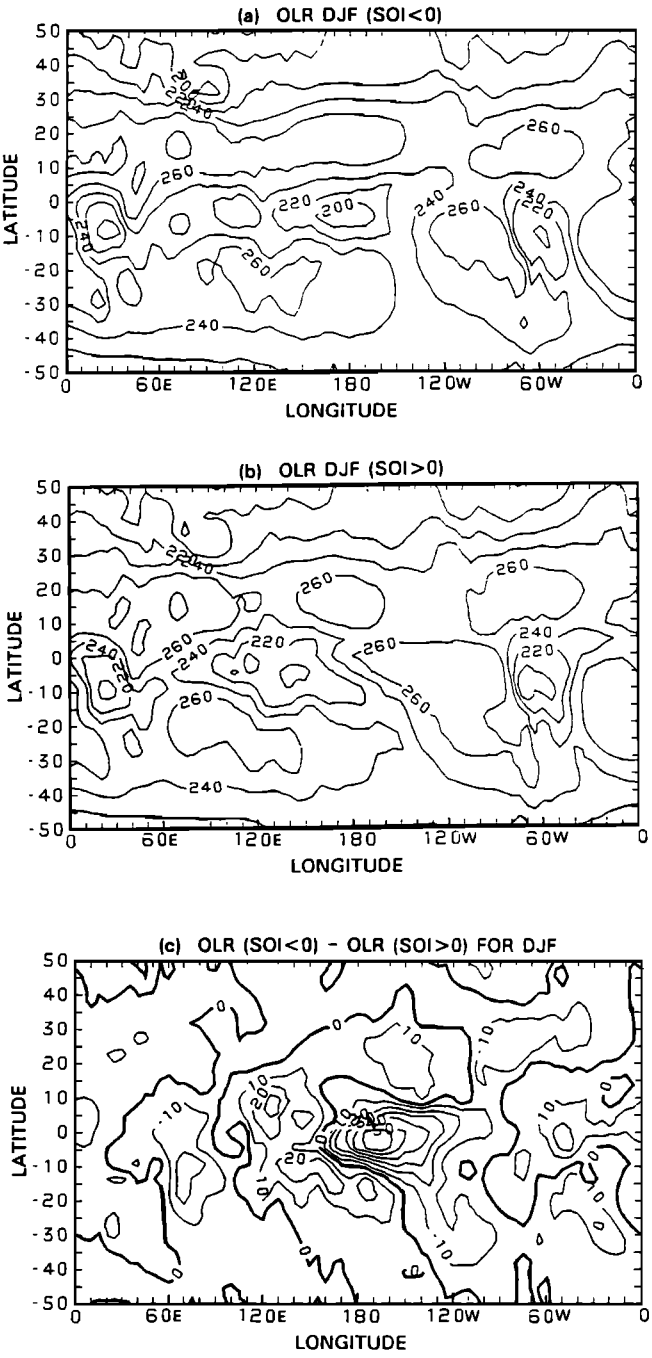

Fig. 4. Latitude-longitude distributions of mean DJF OLR (W m^{-2}) for (a) El Niño (SOI < 0) using the 1982–1983 and 1986–1987 seasonal data, (b) La Niña (SOI > 0) using the 1975–1976 and 1981–1982 seasonal fields and (c) difference between the El Niño and La Niña mean OLR fields. (Units W m^{-2}.)

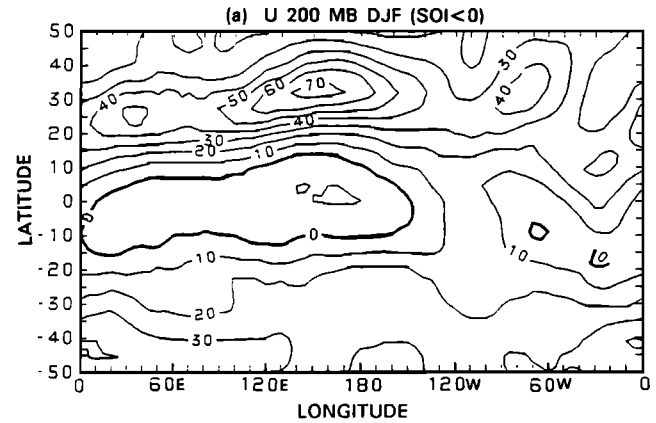

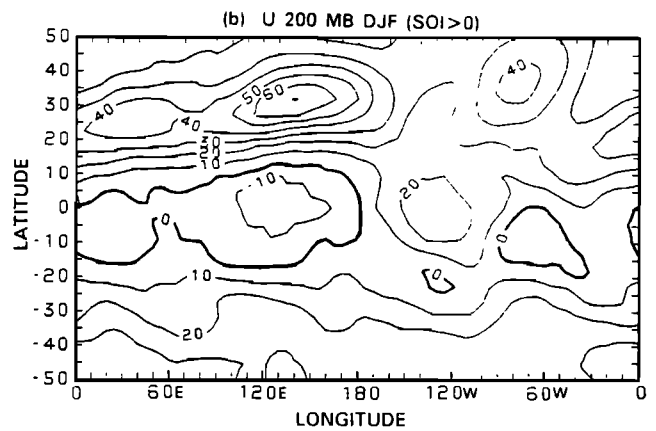

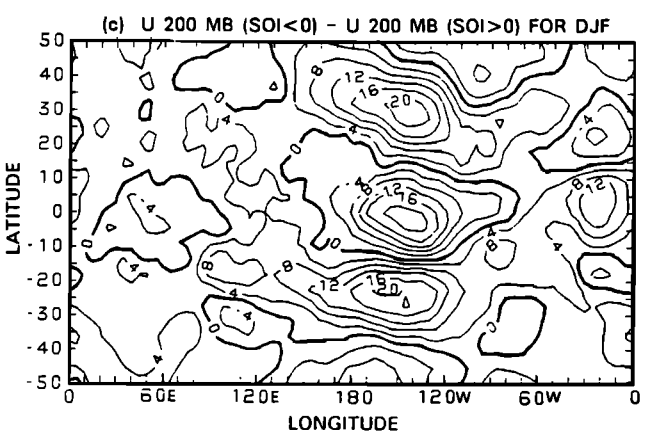

Fig. 5. Longitude–latitude distributions of the 200–mbar zonal wind component, $\bar{U}$, for DJF for (a) El Niño (SOI < 0) using the 1982–1983 and 1986–1987 seasonal data, (b) La Niña (SOI > 0) using the 1975–1976 and 1981–1982 seasonal fields and (c) difference between the El Niño and La Niña mean $\bar{U}$-fields. (Units m s^{-1}.)

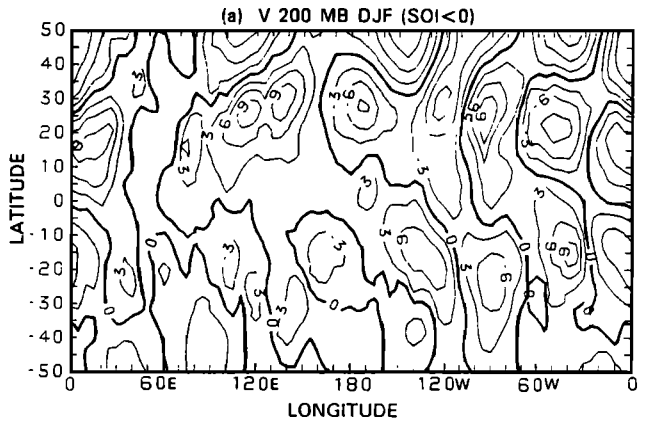

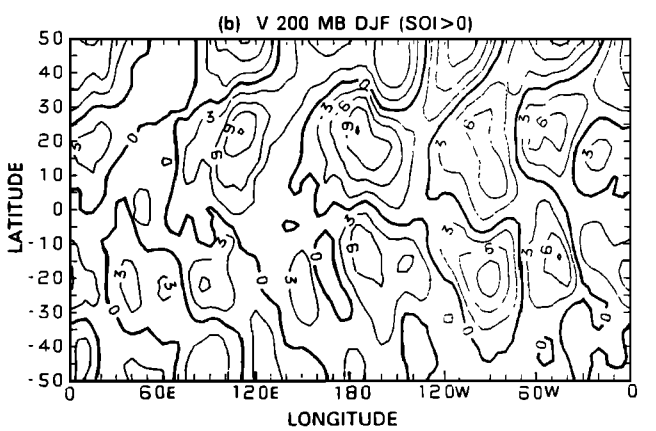

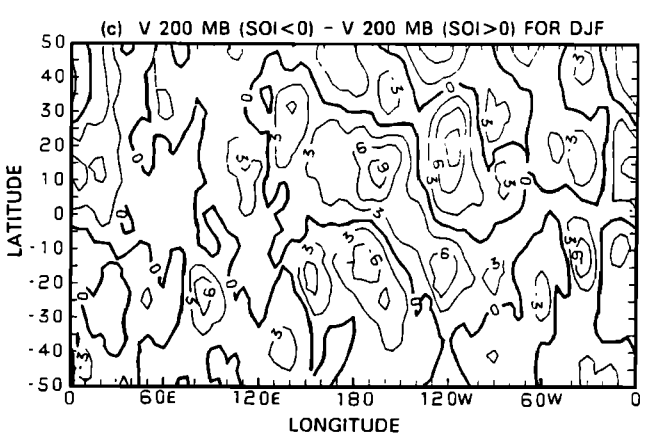

Fig. 6. Longitude–latitude distributions of the 200–mbar meridional wind component, $\bar{V}$, for DJF for (a) El Niño (SOI < 0) using the 1982–1983 and 1986–1987 seasonal data, (b) La Niña (SOI > 0) using the 1975–1976 and 1981–1982 seasonal fields and (c) difference between the El Niño and La Niña mean $\bar{V}$-fields. (Units m s^{-1}.)

Pacific Ocean. These features are consistent with those revealed by Figure 2. Opposite sign but smaller magnitude changes exist over the Atlantic Ocean. We also note that these maximum changes all occur in regions of light shear and where the wind is basically westerly. The maximum values of perturbation kinetic energy (PKE) are usually found within these regions [*Arkin and Webster*, 1985; *Webster and Yang*, 1989].

Figure 6 shows the corresponding distributions of the mean 200–mbar $\bar{V}$ field, whose ENSO-related features have been less emphasized than the $\bar{U}$ field. It can be seen that the magnitude of the interannual variations of the meridional wind is the same order as that of the meridional wind itself, indicating that the eastward shifts in the pattern are substantial. The largest changes occur within the mid-Pacific troughs which decrease in magnitude and shift eastward significantly during El Niño years. Our current study shows that the interannual variability of these troughs is closely associated with distinct changes in PKE, implying that they may play an important role in the atmospheric interaction

between latitudes. Another remarkable feature is the weakening in the meridional wind over East Asia during the El Niño years, which is thought to be a result of the weaker heating over the eastern Indian Ocean and the western Pacific Ocean.

In summary, the interannual variations of the extratropical westerlies, the subtropical meridional wind and the tropical heating are closely linked during ENSO, at least in winter. The eastward displacement of the maximum heating center from Indonesia to the central Pacific Ocean (see Figure 4) is accompanied by an eastward migration of both the maximum meridional wind (Figure 6) and the Asian jet (Figure 5). The locally weakened heating in the Indonesian regions appears to lead to a weaker northward meridional flow or at least an eastward displacement of the maximum meridional flow, which, in turn, may account for the weakening of the Asian jet in the west (upstream of the jet). On the other hand, the increasing latitudinal heating gradient over the central Pacific Ocean may intensify the downstream portion of the jet. (We have become aware that T.C. Chen has recently submitted a paper to the *Journal of Atmospheric Sciences* on a similar topic.)

Figure 7 shows the differences between a number of zonally averaged quantities for years where the SOI >> 0 and SOI << 0. The same years define the curves as those used in Figures 4–6, except in Figure 7c where only the data of DJF of 1981/1982 are used for the La Niña category. From September 1974 through August 1978, the Hough analysis, which uses a spectral representation of the first-guess and data-generated corrections to the spectral coefficients, and which is essentially nondivergent, was used in the NMC analyses [*Arkin*, 1982]. Thus, it will be inappropriate to show the Hadley cell using the zonal mean $\bar{V}$ field from this time period. The discontinuity in the data quality proves to be inconvenient for the composite analyses. However, as stated before, we are forced to live with these deficiencies. During El Niño years, the zonally averaged OLR indicates that the convection is much stronger at low latitudes than during La Niña years (Figure 7a). Furthermore, the tropical easterlies and the winter extratropical westerlies are stronger, and the Hadley cell is stronger

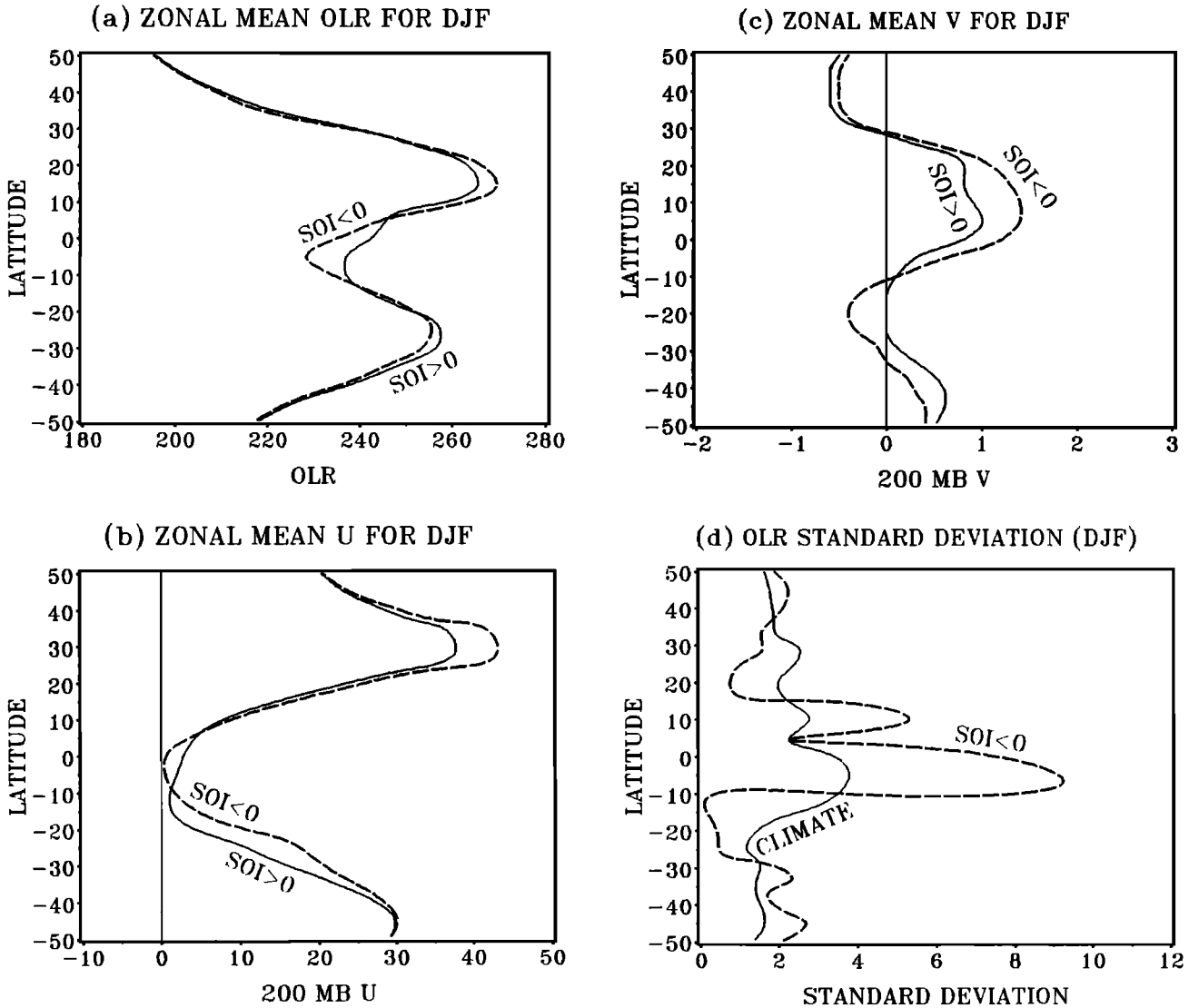

Fig. 7. DJF latitudinal sections of (a) the zonal mean OLR (W m^{-2}), (b) the zonal mean 200-mbar $\bar{U}$-field (m s^{-1}), and (c) the zonal mean 200-mbar $\bar{V}$-field (m s^{-1}). Fields pertaining to positive and negative SOI values are shown as solid and dashed curves, respectively. The DJF OLR standard deviation for climate mean state and the years of SOI < 0 is shown in (d). The same years were used to compute the means as in Figure 4, except in (c) where only DJF of 1981/1982 is used in the La Niña category.

when SOI << 0 compared to SOI >> 0. An indication of the significance of the El Niño deviations from the average can be seen in Figure 7d. Compared to the standard deviation of the OLR for all years, the standard deviation during the El Niño years is very much larger. Clearly, both local and planetary scale differences are evident during the boreal winter through the ENSO cycle.

4.2. *Interannual Variability of OLR, $\bar{U}$, and $\bar{V}$ During Summer*

The OLR, $\bar{U}$ and $\bar{V}$ fields for two El Niño summers (JJA of 1982 and 1987) and two La Niña summers (JJA of 1975 and 1981) are represented in Figures 8, 9 and 10, respectively. The seasonal mean values of the SOI are -3.4, -2.1, 1.9 and 0.9 for the JJA of 1982, 1987, 1975 and 1981, respectively. Generally, the changes of the OLR and wind fields between the El Niño and La Niña summers are similar to the winter differences (Figures 4, 5 and 6) except for a generally smaller magnitude. In particular, when SOI < 0, the diabatic heating over the East Asian monsoon regions and the western Pacific Ocean is weaker and moves southeastward in the summers. Also during such periods, the diabatic heating intensifies along the Intertropical Convergence Zone (ITCZ) over the northern Pacific Ocean but weakens over the Atlantic Ocean.

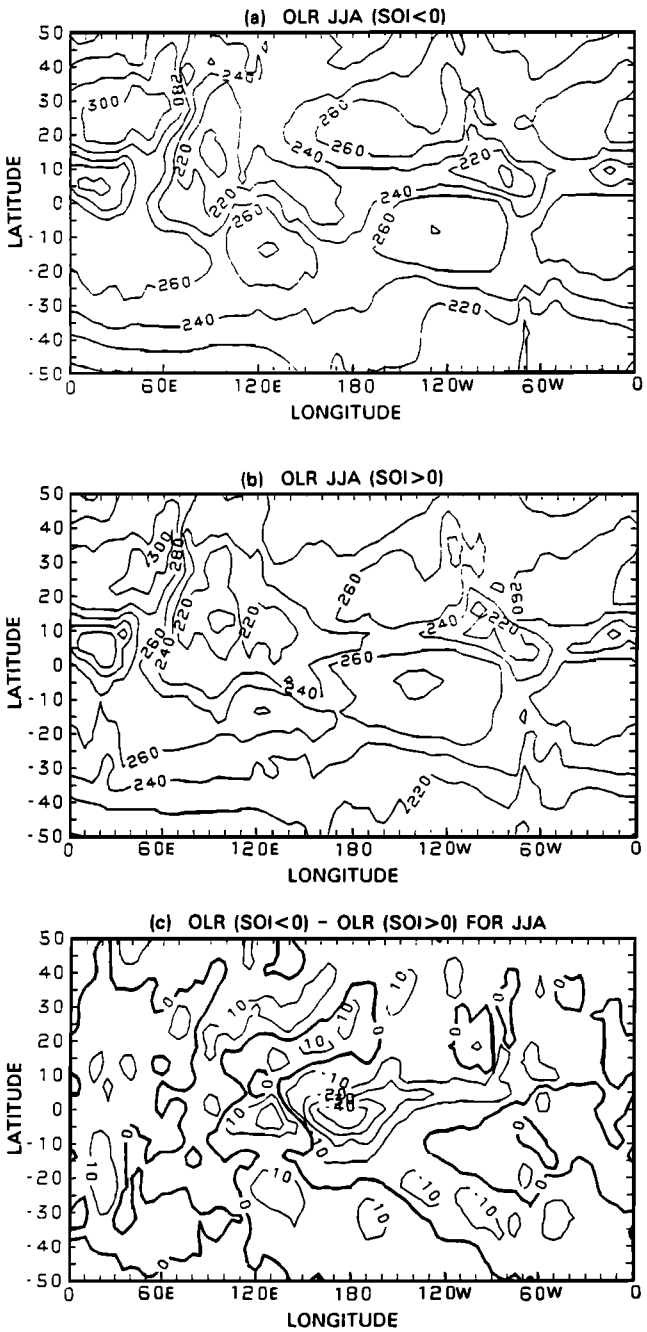

Fig. 8. Latitude-longitude distributions of mean JJA OLR (W m^{-2}) for (a) El Niño (SOI < 0) using the 1982 and 1987 seasonal data, (b) La Niña (SOI > 0) using the 1975 and 1981 seasonal data and (c) difference between the El Niño and La Niña mean JJA OLR fields. (Units wm^{-2}.)

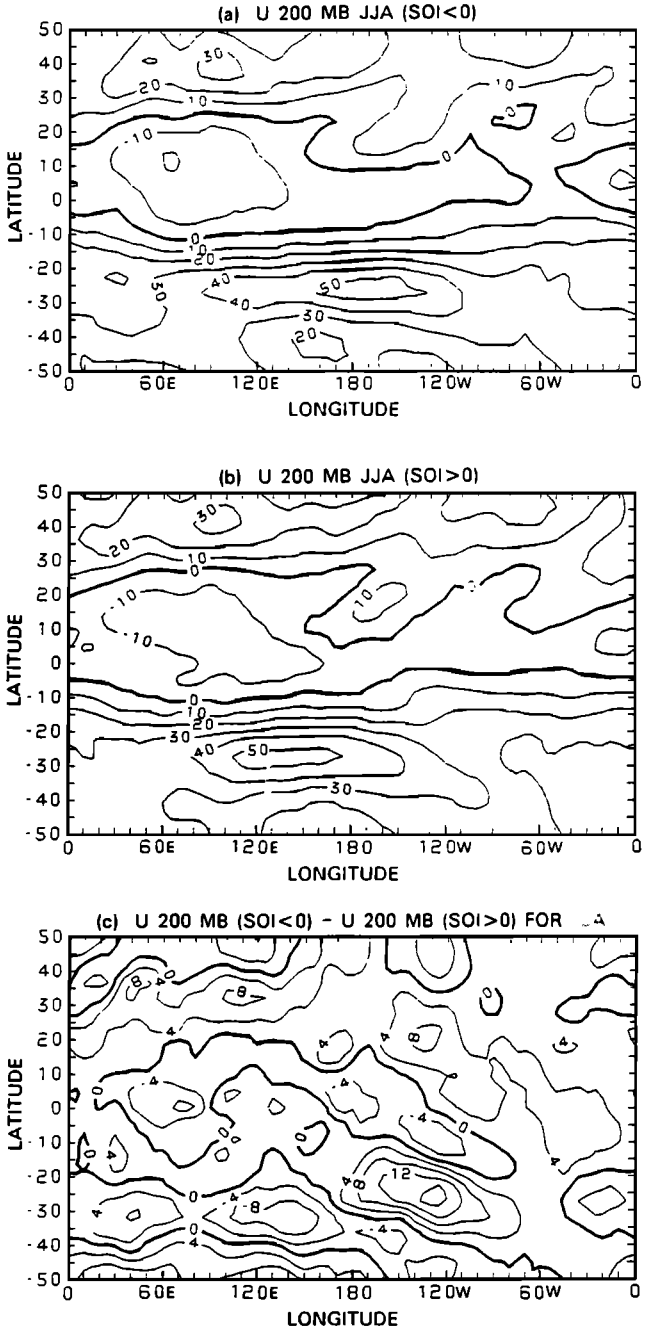

Fig. 9. Longitude–latitude distributions of the 200-mbar zonal wind component, $\bar{U}$, for JJA for (a) El Niño (SOI < 0) using the 1982 and 1987 seasonal data, (b) La Niña (SOI > 0) using the 1975 and 1981 seasonal data and (c) difference between the El Niño and La Niña mean $\bar{U}$-fields. (Units m s^{-1}.)

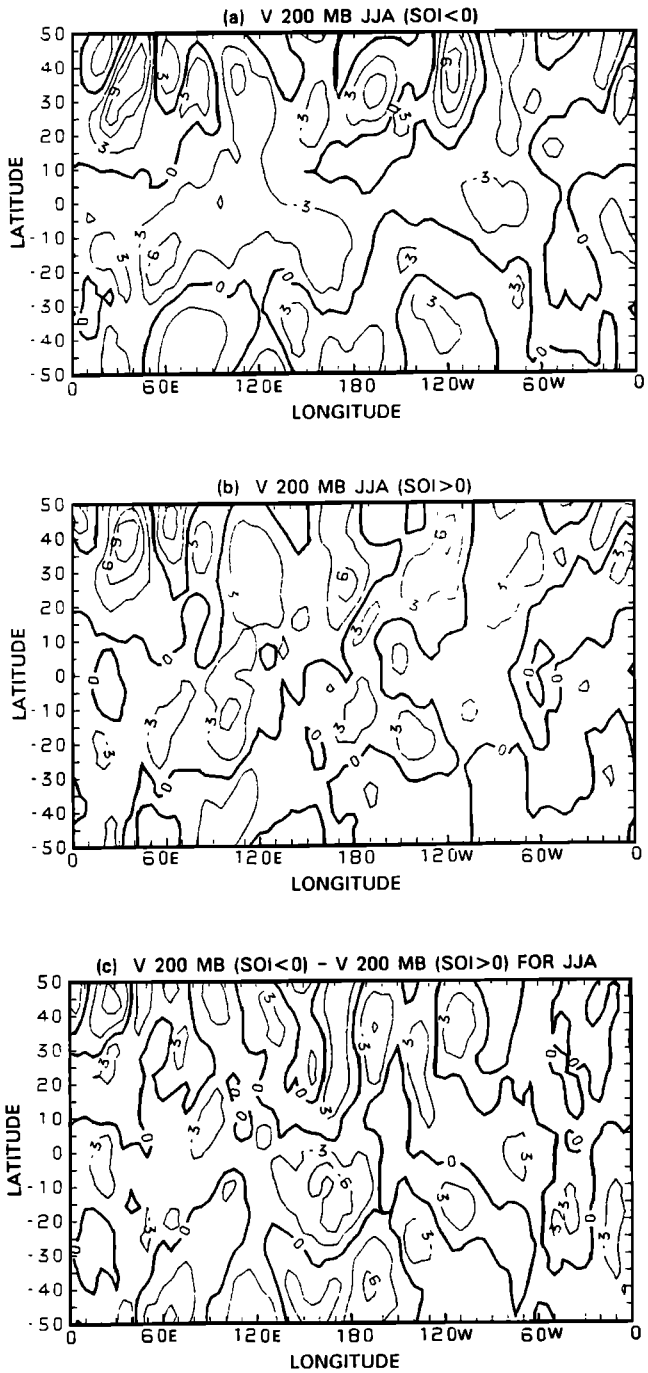

Fig. 10. Longitude–latitude distributions of the 200–mbar zonal wind component, $\bar{V}$, for JJA for (a) El Niño (SOI < 0) using the 1982 and 1987 seasonal data, (b) La Niña (SOI > 0) using the 1975 and 1981 seasonal data and (c) difference between the El Niño and La Niña mean $\bar{V}$-fields. (Units m s^{-1}.)

Furthermore, OLR changes in the extratropical-subtropical Pacific Ocean are out of phase with respect to those in the tropical Pacific Ocean.

Between the SOI extremes, there are large changes in the mean 200–mbar $\bar{U}$ field during the summers (Figure 9). In the tropics, the easterlies become stronger over the Pacific Ocean but weaker over the Atlantic Ocean in El Niño summers, which are consistent with the displacement of the Walker circulation and the heating anomalies shown in Figure 8. When SOI < 0, in the subtropics and extratropics, the westerlies become stronger over the Pacific Ocean, especially in the southern hemisphere. On the other hand, the westerlies become weaker over Australia and the Indian Ocean.

Unlike the situation during DJF, the 200–mbar $\bar{V}$ field (Figure 10) does not show a symmetric structure about the equator during JJA. However, the ENSO related features of the interannual variations of the meridional wind during JJA are still similar to those during DJF. Figure 10 indicates that there are more negative meridional winds in the tropics during El Niño summers than La Niña summers, reflecting a stronger overturning when SOI < 0. The stronger overturning may be seen in the OLR distributions in Figure 8. In the subtropics, the meridional wind patterns migrate eastward significantly in the El Niño summers, especially in the southern hemisphere. Besides the shift in the mid-Pacific troughs, as in DJF, a remarkable weakening and eastward migration of the northerly wind occurs over the eastern Indian Ocean, which may be responsible for the distinct upstream weakening of the Australian jet stream.

In summary, the interannual anomalies of the Asian monsoon heating, the southern hemisphere subtropical meridional wind and the Australian jet stream during JJA are similar to those occurring during DJF. However, two important differences should be pointed out. First, the upstream weakening of the Australian jet during JJA is more significant than the upstream weakening of the Asian jet during DJF. Second, the eastward displacement of the Australian jet is also more distinct. Thus, by inference, it might be expected that the location and intensity of the Australian jet stream may be affected more by tropical heating than the Asian jet stream.

Figure 11 shows the differences of some zonally averaged quantities, specifically, the OLR, the 200–mbar zonal velocity component and the 200–mbar meridional velocity component. Because of the discontinuity of data quality, as discussed in section 4.1, only the data of JJA of 1981 are used in Figure 11c for the La Niña category. For most fields, the differences between El Niño and La Niña for JJA are far smaller than those which exist for DJF, as shown in Figure 7. The exceptional field is the meridional velocity component (Figure 11c) which is much stronger in El Niño times. The difference seems to overreflect the slightly enhanced convection occurring in the tropics. Indeed, Figure 11d shows that the deviation of the OLR during El Niño summers is only slightly greater than the regular interannual variance.

5. YEAR-TO-YEAR VARIABILITY OF TROPICAL HEATING AND EXTRATROPICAL JET STREAMS

In order to assess a more general interannual relationship between the summer hemisphere tropical heating and the winter hemisphere extratropical jets, which may or may not be associated with the ENSO cycle, the evolution of the seasonal mean fields are examined.

5.1. *Evolution of OLR, $\bar{V}$, and $\bar{U}$ During Winter*

Figure 12 depicts the year-to-year variations of the mean (0-10°S) OLR, the 200–mbar mean (15°N-25°N) meridional wind and the 200–mbar mean (30°N-40°N) zonal wind for DJF in the form of longitude-time plots. The seasonal mean values of the SOI are displayed on the right-hand ordinate of each diagram. The three particular variables were chosen because of their pertinence to the hypothesized interhemispheric relationships determined using input from Figures 4–6. The latitude belts were

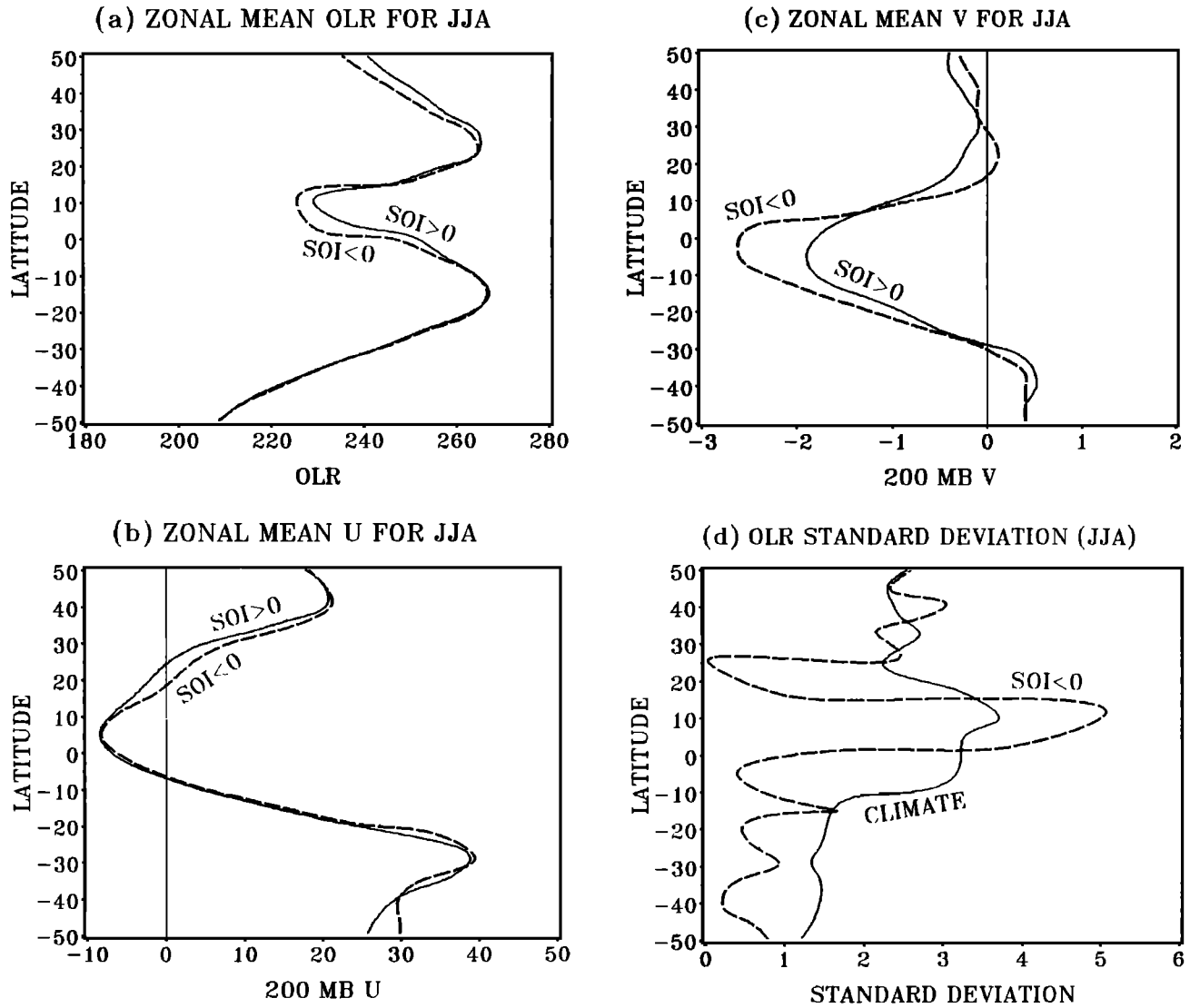

Fig. 11. JJA latitudinal sections of (a) the zonal mean OLR (W m^{-2}), (b) the zonal mean 200–mbar $\bar{U}$-field (m s^{-1}) and (c) the zonal mean 200–mbar $\bar{V}$-field (units m s^{-1}). Fields pertaining to positive and negative SOI values are shown as solid and dashed curves, respectively. The JJA OLR standard deviation for climate mean state and the years of SOI < 0 is shown in (d). The same years were used to compute the means as in Figure 8, except in (c) where only JJA of 1981 is used in the La Niña category.

chosen to match the regions of maximum heating, the belt of maximum cross-equatorial flow and the zone of the maximum winter westerlies.

Figure 12 shows that the Asian jet stream becomes stronger when the heating center near Indonesia becomes stronger [i.e., smaller OLR]. In the winters of 1969/1970, 1974/1975, 1976/1977, 1980/1981 and 1983/1984, the jet is relatively stronger (A, B, C, D, and E in Figure 12c). Also in these winters, the subtropical meridional winds [i.e., the southerly wind upstream and the northerly wind downstream of the jet] are correspondently stronger. It can be seen from Figure 12a that the OLR values in Indonesian are smaller during the DJF of 1976/1977, 1979/1980 - 1981/1982, and 1983/1984 - 1985/1986. Thus, the stronger Asian jet and meridional winds appear to be associated with the stronger diabatic heating over the Indonesian regions in winter. Conversely, it seems that there is a correspondence between the weaker heating (larger OLR) and the weaker Asian jet through a weaker cross-equatorial meridional wind. Also, it appears that the eastward movement of the Asian jet in the winters of 1969/1970, 1972/1973, 1977/1978, 1982/1983, and 1986/1987 seems to be associated with the eastward migration of the maximum heating over Indonesia.

So far, we have not discussed the ENSO-related features of the year-to-year variations of the Asian jet stream shown in Figure 12. Several features can be discerned: (1) the downstream strengthening (weakening) of the jet occurs in the winters when SOI < 0 (SOI ≥ 0); (2) most major El Niño (La Niña) winters are accompanied by downstream strengthening (weakening) of the Asian jet stream. Thus, a very clear ENSO relationship exists in the interannual variability of the downstream portion of the Asian jet. On the other hand, the upstream strengthening (weakening) of the jet does not appear to occur in the major El Niño (La Niña) winters. These ENSO relationships of the jet stream, listed above, are shown more clearly in Figure 13 which represents a

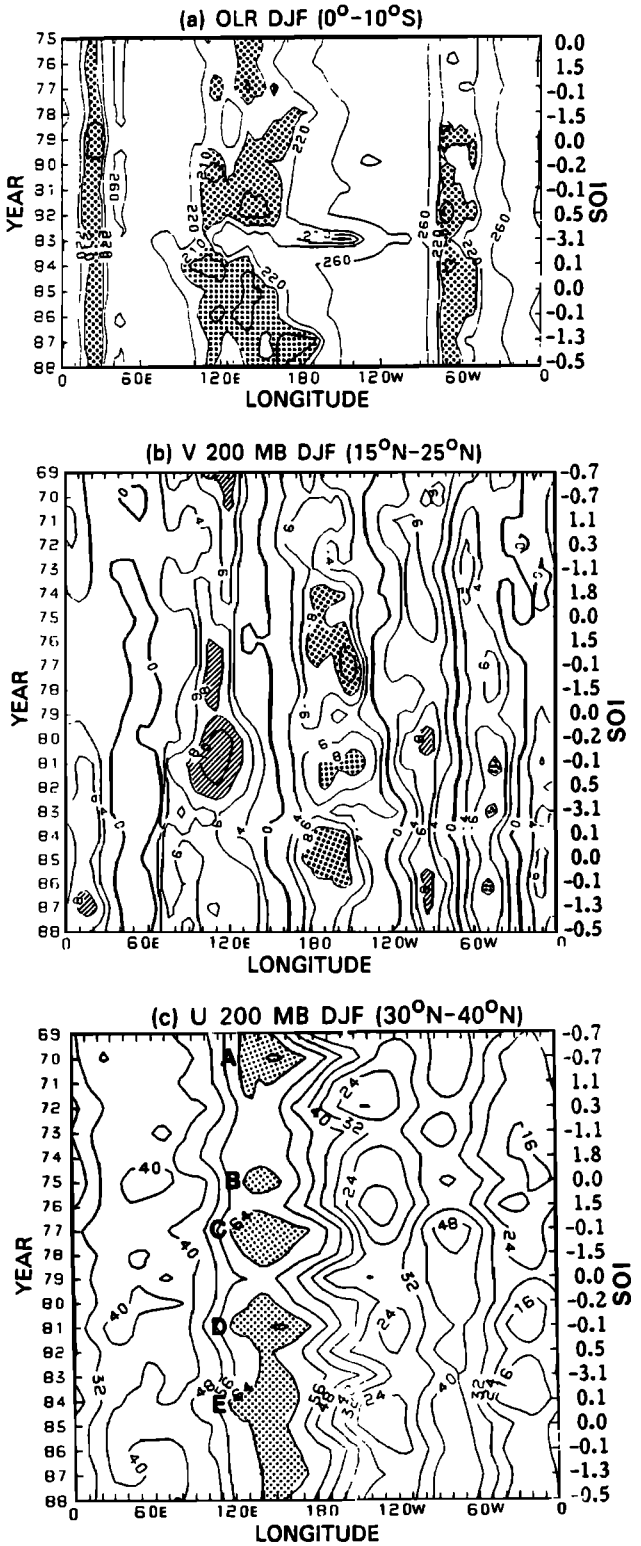

Fig. 12. Longitude-time representation of interannual variations for DJF of (a) OLR (W m^{-2}) averaged between 0° and 10°S, (b) 200-mbar meridional wind component (m s^{-1}) averaged between 15°N and 25°N and (c) 200-mbar zonal wind component (m s^{-1}) averaged between 30°N and 40°N. The mean values of the SOI are shown for each DJF on the right hand side of the diagrams. The DJF of 1968/1969, 1969/1970 and 1970/1971 and so on is represented by 69, 70 and 71 and so on. Areas of OLR < 210 W m^{-2}, V < –8 m s^{-1} and U > 64 m s^{-1} are stippled in (a), (b) and (c), respectively. Areas of V > 8 m s^{-1} are hatched in (b).

composite of the three quantities shown in Figure 12. It should be pointed out that Figure 13 mainly summarizes the features shown in Figure 12 which presents a more general heating-jet-ENSO relationship than the discussion in section 4. Thus, compared with Figs. 4–7, more El Niño years (1972/1973 and 1977/1978) and La Niña years (1970/1971 and 1973/1974) are added to the wind field in Figure 13 for the purpose of obtaining, as closely as possible, the most accurate general picture. In each panel, the El Niño and La Niña curves are labeled. The most obvious

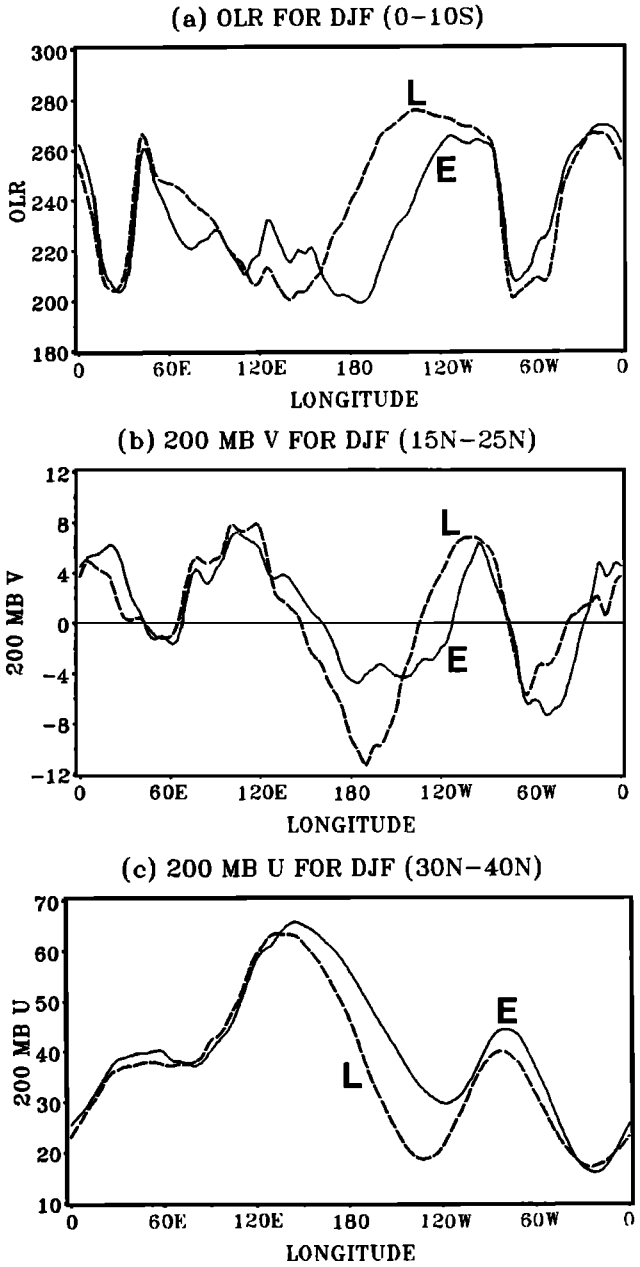

Fig. 13. Longitudinal distribution of composite DJF distributions of SOI < 0 (El Niño, labeled E: solid lines) and SOI > 0 (La Niña, labeled L: dashed lines) of (a) the mean OLR between 0°–10°S, (b) the mean 200-mbar $\bar{V}$ averaged between 15°N-25°N and (c) the mean 200-mbar $\bar{U}$ averaged between 30°N-40°N. The SOI < 0 data were the DJF seasonal averages of 1982/1983 and 1986/1987 for the OLR data. 1972/1973 and 1977/1978 were also used for the $\bar{U}$ and $\bar{V}$ composites. The SOI > 0 data comprised the 1975/1976 and 1981/1982 for the OLR plus 1970/1971 and 1973/1974 for the dynamic fields.

changes in the composite are the general eastward shift of the convection (Figure 13a) in the western and central Pacific Ocean during El Niño. Over the western Indian Ocean the convection is also more intense. However, over the remainder of the tropics, moderately larger values (reduced convection) appear with the largest values over the eastern Indian Ocean and Indonesia. Note that the change of the jet core and westerlies to its west are relatively small. Apparently, the westerlies to the east increase instead. Thus, the increase in the strength of the westerlies over the western hemisphere is most responsible for the change in the magnitude of the zonally averaged $\bar{U}$-field and this can be ascribed directly to the change in the meridional flow associated with the heating. With the anomalous increase of convection to the south of the equator, the southward flow over the central North Pacific Ocean is reduced.

5.2. *Evolution of OLR, $\bar{V}$, and $\bar{U}$ During Summer*

Figure 14 depicts the year-to-year variations of the mean (10°N-20°N) OLR, the 200–mbar mean (15°S and 25°S) meridional wind and the 200–mbar mean (25°S and 35°S) zonal wind for JJA. The OLR data are averaged between 10°N and 20°N in order to represent the interannual oscillations in the monsoon heating. The seasonal mean values of the SOI are shown on the right hand side of the diagrams for each JJA.

A heating-jet association, similar to that revealed in Figure 12, appears in Figure 14. During the JJA of 1974, 1978, 1981 and 1986, the Australian jet stream is relatively stronger (A, B, C, and D in Figure 14c). (Figure 14c is identical to the lower panel of Figure 2b. It is shown here for completeness and easy comparison with Figures 14a and 14b.) At the same time, the subtropical northerly wind upstream and southerly wind downstream of the jet are relatively stronger as well. At a first glance, it seems that the correspondence between the stronger jet and Asian monsoon heating is not so clear. However, a more careful examination of Figure 14a shows that the diabatic heating east of 110°E is relatively stronger when the jet is stronger (e.g., the JJA of 1981 and 1986). On the other hand, weaker jet and subtropical winds appear to be linked to weaker Asian monsoon heating.

Figure 14b shows that the subtropical meridional winds shift eastward significantly in the summers when the SOI << 0. It appears that the movement of the maximum meridional flow is about 70-90°E of longitude. Consistently, the Australian jet stream moves eastward as well (e.g., the JJA of 1972, 1977, 1982 and 1987, shown in Figure 14c). In summary, the eastward movement of the jet and the meridional winds seems to be associated with the eastward extension of the Asian monsoon heating.

By comparing Figures 12 and 14, it is apparent that the changes of the Australian jet stream are more related to the ENSO cycle than the Asian jet. Significant downstream strengthening (weakening) of the Australian jet occurs in the El Niño (La Niña) years, and the westerlies at the upstream portion (e.g., 120°E) are weaker (stronger) in the El Niño (La Niña) years. These features are summarized by the composites shown in Figure 15. During the El Niño years, the Australian jet stream moves eastward significantly when the subtropical meridional winds (the poleward winds over the southern Indian Ocean and the eastern Pacific Ocean, and the equatorward winds over the central Pacific Ocean) shift eastward and decrease in magnitude. These changes appear to be associated with the eastward migration of the heating in the other hemisphere. It is worthy re-emphasizing that the upstream weakening of the Australian jet in the El Niño years is more distinct than the Asian jet in DJF and that the changes in the meridional winds over the Pacific Ocean reflect the changes in the mid-Pacific trough.

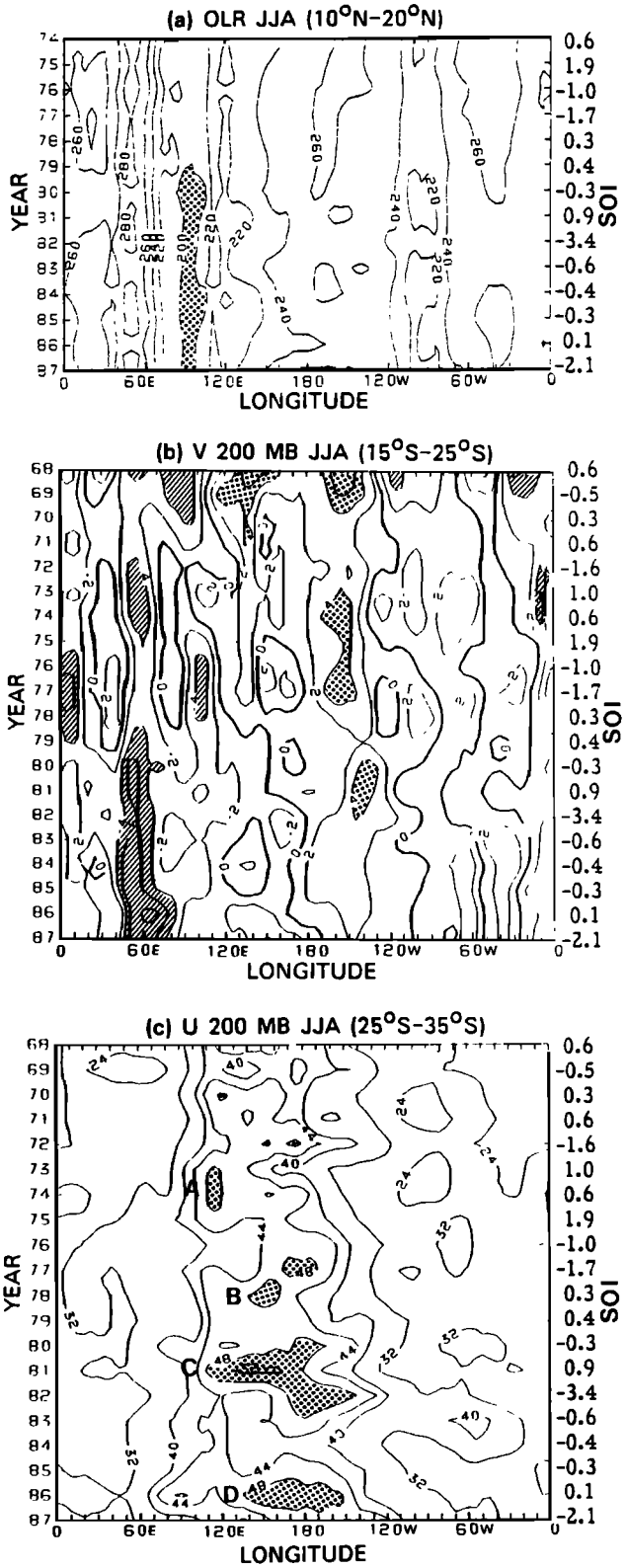

Fig. 14. Longitude-time representation of interannual variations for JJA of (a) OLR (W m^{-2}) averaged between 10°N and 20°N, (b) 200–mbar meridional wind component (m s^{-1}) averaged between 15° S and 25°S and (c) 200–mbar zonal wind component (m s^{-1}) averaged between 25°S and 35°S. The mean values of the SOI are shown for each JJA on the right hand side of the diagram s. Areas of OLR < 200 W m^{-2}, V > 4 m s^{-1} and U > 48 m s^{-1} are stippled in (a), (b) and (c), respectively. Areas of V < –4 m s^{-1} are hatched in (b).

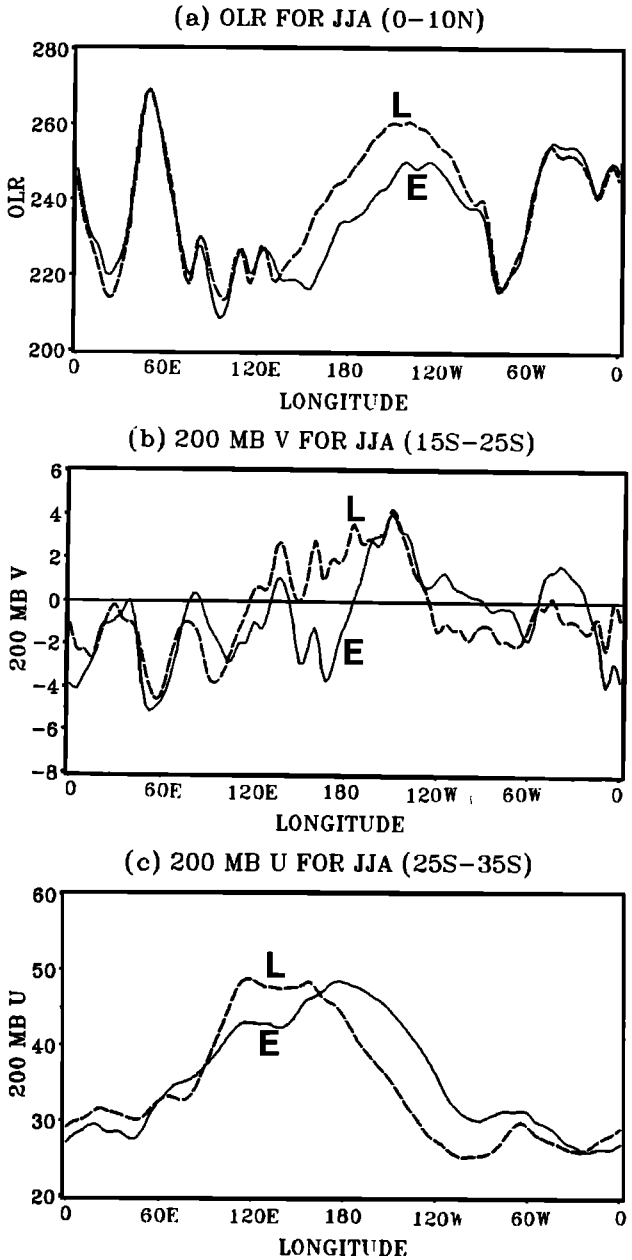

Fig. 15. Longitudinal distribution of composite JJA distributions of SOI < 0 (El Niño, labeled E: solid lines) and SOI >0 (La Niña, labeled L: dashed lines) of: (a) the mean OLR between 0°–10°N, (b) the mean 200–mbar $\bar{V}$ averaged between 15°S-25°S and (c) the mean 200–mbar $\bar{U}$ averaged between 25°S-35°S. The SOI < 0 data were the JJA seasonal averages of 1977, 1982 and 1987 for the OLR data. 1972 was also used for the $\bar{U}$ and $\bar{V}$ composites. The SOI > 0 data comprised the 1974, 1975 and 1981 for the OLR plus 1971 for the dynamic fields.

6. CONCLUSIONS

The main results obtained in this study are summarized as follows:

1. The extratropical westerly jet streams in the winter hemisphere are poleward of the tropical OLR minima in the summer hemisphere. During DJF, the jets over Asia, North America and Europe are associated in longitude with the heating maxima over Indonesia, South America, and South Africa, respectively. During JJA, the jet maxima over Australia, South America, and South Africa are associated with the heating maxima over the Asian monsoon regions, North America and North Africa, respectively. With a considerably more extensive data set, we find the hypothesis of *Krishnamurti* [1979] essentially correct.

2. The location of the major southern hemisphere winter jet stream is keenly associated with the location of the cross-equatorial flow from the convective heating regions of East Asia. Thus, we have generalized Krishnamurti's association between summer heating and the winter jet streams to the southern hemisphere.

3. The annual changes of the intensity of the extratropical westerly jets in the winter hemisphere are in phase with those of the three maximum heating centers in the tropics in the summer hemisphere.

4. The variations of the extratropical westerly jet streams, the subtropical meridional wind in the winter hemisphere and the tropical heating in the summer hemisphere are closely associated on an interannual time scale. The tropical heating is important in controlling the year-to-year oscillations of the extratropical westerly jet streams.

5. The generalization of the association of the summer heating and the winter jet streams questions the generality of the association between extratropical jet streams and the major orographic features suggested by *Wallace* [1983].

6. When the heating is stronger in the Australian monsoon regions during DJF, the subtropical poleward wind becomes stronger. This leads to a stronger extratropical westerly jet stream over Asia at a relatively west location and stronger equatorward wind over the northern central Pacific Ocean. As the stronger heating in those regions increases the longitudinal heating gradient between the western and central Pacific Ocean, the equatorial westerlies become stronger. It can be seen from Figure 2, in which the interannual variations of the 200–mbar U field averaged between 5°S and 5°N for DJF and JJA are shown, that during DJF, both the easterlies over the Indonesian regions and the westerlies over the central Pacific Ocean become stronger when the heating is stronger over Indonesia. When the maximum heating center moves eastward and the heating locally weakens in the Australian monsoon regions, the poleward wind becomes weaker and shifts eastward. This may lead to an upstream weakening of the jet when the tropical heating weakens significantly. As the eastward migration of heating increases the latitudinal heating gradient in the central Pacific Ocean, a significant downstream strengthening of the jet may be found. At the same time, the warming of the central Pacific Ocean is accompanied by a weakening equatorward wind in those longitudes over the North Pacific. The Australian monsoon heating and Asian jet stream association is related to the ENSO cycle, especially the changes in the downstream portion of the jet, and is shown in Figure 16a.

7. When the heating is stronger in the Asian monsoon regions (especially East Asia) in JJA, the extratropical westerly jet stream over Australia and the subtropical meridional winds over the southern Indian Ocean and the central Pacific Ocean become stronger. When the maximum heating moves eastward and the heating weakens in the Asian monsoon regions, the meridional winds become weaker and shifts eastward. This leads to a remarkable upstream weakening and a significant downstream strengthening of the Australian jet stream together with a weakening equatorward wind over the Southern Central Pacific Ocean. The Asian monsoon heating and Australian jet stream association, stronger than the association between the Australian monsoon heating and

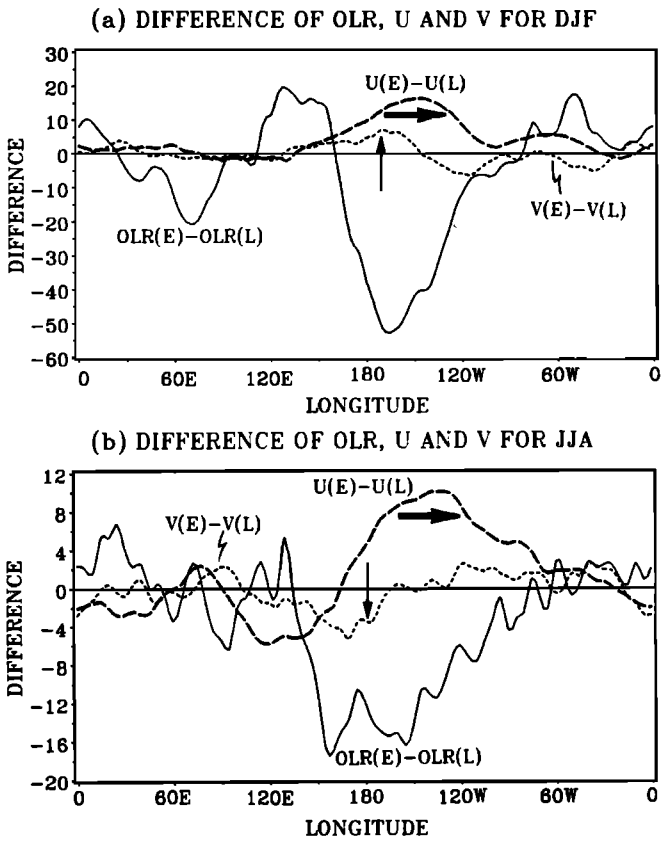

Fig. 16. Difference fields (i.e., El Niño minus La Niña) of OLR, 200-mbar V and 200-mbar U for (a) DJF and (b) JJA. The differences in (a) are calculated from Figure 13 where the OLR, V and U are averaged between 0°–10°S, 15°N–25°N and 30°N–40°N, respectively. The differences in (b) are calculated from Figure 15 where the OLR, V and U are averaged between 0°–10°N, 15°S–25°S and 25°S–35°S, respectively. The thick arrows indicate the eastward migration and downstream strengthening of the jets; the thin arrows indicate the eastward migration and weakening of the subtropical meridional winds.

the Asian jet in DJF, and more closely related to the ENSO cycle, is shown in Figure 16b.

The study has been undertaken with the use of seasonal averages. It would be interesting to see if the associations between the summer heating variations and the winter jet streams elucidated in this study are apparent on shorter time scales. There is considerable evidence that the heating over the tropical warm pool regions undergoes strong variations on submonthly time scales [*Chang and Webster*, 1989]. If this proved to be true, it would seem to have considerable significance for medium range weather forecasting. To test the association, we are currently analyzing data archived from the ECMWF model. We are also planning a series of experiments with the NMC global spectral model.

Acknowledgements. This report was supported by NSF Grants ATM 83-18852 and ATM 87-03267. Computing was carried out at the National Center for the Atmospheric Research and at the Pennsylvania State University. We are appreciative of the Monsoon Program of the US-PRC Protocol in Atmospheric Science which supported S. Yang during the early period of his tenure at the Pennsylvania State University. We would like to thank H.-R. Chang of the Pennsylvania State University for many stimulating discussions and P. A. Arkin of the NMC Climate Analysis Center for the provision of the data used in this study. We would also like to thank Lisa Davis for her careful editing of this manuscript.

REFERENCES

Arkin, P.A., The relationship between interannual variability in the 200 mb tropical wind field and the Southern Oscillation, *Mon. Weather Rev.*, *110*, 1393-1404, 1982.

Arkin, P.A., and P.J. Webster, Annual and interannual variability of tropical-extratropical interaction: An empirical study, *Mon. Weather Rev.*, *113*, 1510-1523, 1985.

Bjerknes, J., A possible response of the atmospheric Hadley circulation to equatorial anomalies of ocean temperature, *Tellus*, *18*, 820-829, 1966.

Bjerknes, J., Atmospheric teleconnections from the equatorial Pacific, *Mon. Weather Rev.*, *97*, 163-172, 1969.

Blackmon, M.L., J.M. Wallace, N.-C. Lau and S.L. Mullen, An observational study of the Northern Hemisphere wintertime circulation, *J. Atmos. Sci.*, *34*, 1040–1053, 1977.

Bolin, B., On the influence of the earth's orography on the general character of the westerlies, *Tellus*, *2*, 184-196, 1950.

Chang, C.-P., Viscous internal gravity waves and low frequency oscillations in the tropics, *J. Atm. Sci.*, *34*, 901–910, 1977.

Chang, H.-R., and P.J. Webster, Energy accumulation and emanation at low latitudes. Part II: Nonlinear response to strong episodic equatorial forcing, *J. Atmos. Sci.*, in press, 1989.

Charney, J.G., and A. Eliassen, A numerical method for predicting the perturbations of the middle latitude westerlies, *Tellus*, *1*, 38-54, 1949.

Chen, C.-S., and K.E. Trenberth, Forced planetary waves in the northern hemisphere winter: Wave coupled orographic and thermal forcing, *J. Atmos. Sci.*, *45*, 682–704, 1988.

Frederiksen, J., and P.J. Webster, Alternative theories of atmospheric teleconnections and low-frequency fluctuations, *Rev. Geophysics*, *26*, 459–494, 1988.

Held, I.M., Stationary and quasi-stationary eddies in the extratropical troposphere: Theory, in *Large-Scale Dynamical Processes in the Atmosphere*, edited by B.J. Hoskins and P.R. Pearce, pp. 127-167, 1983.

Hoskins, B.J., and D.J. Karoly, The steady linear response of a spherical atmosphere to thermal and orographic forcing, *J. Atmos. Sci.*, *38*, 1179-1196, 1981.

Jacqmin, D., and R.S. Lindzen, The causation and sensitivity of the northern winter planetary waves, *J. Atmos. Sci.*, *42*, 724-745, 1985.

James, I.N., On the forcing of planetary-scale Rossby waves by Antarctica, *Q. J. R. Meteorol. Soc.*, *114*, 619–637, 1988.

Kasahara, A., and W.M. Washington, General circulation experiments with a six-layer NCAR model, including orography, cloudiness and surface temperature calculations, *J. Atmos. Sci.*, *28*, 657-701, 1971.

Krishnamurti, T.N., 1979: *Compendium of Meteorology*, vol. 2, part 4–Tropical Meteorology, *Rep.* 364, World Meteorological Organization, Geneva, Switzerland, 1979.

Krishnamurti, T.N., M. Kanamitsu, W.J. Koss and J.D. Lee, Tropical east-west circulation during the northern winter, *J. Atmos. Sci.*, *30*, 780-787, 1973.

Lau, K.M., and J.S. Boyle, Tropical and extratropical forcing of the large-scale circulation: A diagnostic study, *Mon. Weather Rev.*, *115*, 400–428, 1987

Manabe, S., and T.B. Terpstra, The effect of mountains on the general circulation of the atmosphere as identified by numerical experiment, *J. Atmos. Sci.*, *31*, 3-42, 1974.

Opsteegh, J.D., and H.M. van den Dool, Diagnostic study of the time-mean atmosphere over northwestern Europe during winter, *J. Atmos. Sci.*, *36*, 1862–1879, 1980.

Paegle, J., J.N. Paegle, F.P. Lewis and A.J. McGlasson, Description and interpretation of planetary flow structure of the winter 1976 DST data, *Mon. Weather Rev.*, *107*, 1506-1514, 1979.

Ramage. C., Role of the tropical "maritime continent" in the atmospheric circulation, *Mon. Weather Rev.*, *96*, 365–370, 1968.

Ramanathan, V., The role of earth radiation budget studies in climate and general circulation research, *J. Geophys. Res.*, *92*, 4075-4095, 1987.

Rong-hui, H., and K. Gambo, The response of a hemispheric multilevel model atmosphere to forcing by topography and stationary heat sources, *J. Meteorol. Soc. Japan*, *60*, 78-108, 1982.

Sadler, J.C., Mean Cloudiness and Gradient Level Charts over the Tropics, *Tech. Rep. 215*, 63 pp. Air Weather Service [MAC], U. S. Air Force, 1970

Simmons, A. J., The forcing of stationary wave motion by tropical diabatic heating, *Q. J. R. Meteorol. Soc.*, *108*, 503-534, 1982.

Smagorinsky, J., The dynamical influence of large-scale heat sources and sinks in the quasi-stationary mean motions of the atmosphere, *Q. J. R. Meteorol. Soc.*, *79*, 342–366, 1953.

Streten, N.A., Some characteristics of satellite-observed bands of persistent cloudiness over the southern hemisphere, *Mon. Weather Rev.*, *101*, 486-495, 1973.

Trenberth, K.E., and J.G. Olson, An evaluation and intercomparison of global analyses from the National Meteorological Center and the European Centre for Medium Range Weather Forecasts, *Bull. Am. Meteorol. Soc.*, *69*, 1047–1057, 1988.

Wallace, J.M., The climatological mean stationary waves: Observational evidence, in *Large-Scale Dynamical Processes in the Atmosphere* edited by B.J. Hoskins and P.R. Pearce, pp. 27-52, 1983.

Walker, G.T., World Weather II, in *Memories of the Indian Meteorological Department*, vol. *24*, part 9, Indian Meteorological Department, 1924.

Webster, P.J., Temporal variations of low-latitude zonal circulations, *Mon. Weather Rev.*, *101*, 803–816, 1973.

Webster, P.J., Mechanisms determining the atmospheric response to sea surface temperature anomalies, *J. Atmos. Sci.*, *38*, 554-571, 1981.

Webster, P.J., Seasonality in the local and remote atmospheric response to sea surface temperature anomalies, *J. Atmos. Sci.*, *39*, 41-52, 1982.

Webster, P.J., and H.-R. Chang, Equatorial energy accumulation and emanation regions: Impact of a zonally varying basic state, *J. Atmos. Sci.*, *45*, 803–829, 1988.

Webster, P.J., and J.R. Holton, Cross-equatorial response to middle-latitude forcing in a zonally varying basic state, *J. Atmos. Sci.*, *39*, 722–733, 1982.

P.J. Webster, Department of Meteorology, College of Earth and Mineral Sciences, Penn State University, 518 Walker Building, University Park, PA 16802.

Song Yang, Atmospheric and Environmental Research, Inc., 840 Memorial Drive, Cambridge, MA 02139.

(Received December 8, 1989;
revised April 6, 1990;
accepted May 18, 1990.)